Quaternary Science Reviews 130 (2015) 57–71

Contents lists available at ScienceDirect

Quaternary Science Reviews

journal homepage: www.elsevier.com/locate/quascirev

Orbital forcing of glacial/interglacial variations in chemical weathering and silicon cycling within the upper White Nile basin, East Africa: Stable-isotope and biomarker evidence from Lakes Victoria and Edward

Helen E. Cockerton [a], F. Alayne Street-Perrott [a, *], Philip A. Barker [b], Melanie J. Leng [c, d], Hilary J. Sloane [c], Katherine J. Ficken [a]

[a] Department of Geography, College of Science, Swansea University, Swansea, SA2 8PP, UK
[b] Lancaster Environment Centre, Lancaster University, Lancaster, LA1 4YQ, UK
[c] NERC Isotope Geosciences Facilities, British Geological Survey, Nottingham, NG12 5GG, UK
[d] Centre for Environmental Geochemistry, School of Geography, University of Nottingham, Nottingham, NG7 2RD, UK

ARTICLE INFO

Article history:
Received 9 March 2015
Received in revised form
11 July 2015
Accepted 29 July 2015
Available online 21 August 2015

Keywords:
Late Quaternary
White Nile
Lake Victoria
Lake Edward
Silicon cycle
Diatoms
Oxygen isotopes
Silicon isotopes
Biomarkers

ABSTRACT

On Quaternary time scales, the global biogeochemical cycle of silicon is interlocked with the carbon cycle through biotic enhancement of silicate weathering and uptake of dissolved silica by vascular plants and aquatic microalgae (notably diatoms, for which Si is an essential nutrient). Large tropical river systems dominate the export of Si from the continents to the oceans. Here, we investigate variations in Si cycling in the upper White Nile basin over the last 15 ka, using sediment cores from Lakes Victoria and Edward. Coupled measurements of stable O and Si isotopes on diatom separates were used to reconstruct past changes in lake hydrology and Si cycling, while the abundances of lipid biomarkers characteristic of terrestrial/emergent higher plants, submerged/floating aquatic macrophytes and freshwater algae document past ecosystem changes. During the late-glacial to mid-Holocene, 15–5.5 ka BP, orbital forcing greatly enhanced monsoon rainfall, forest cover and chemical weathering. Riverine inputs of dissolved silica from the lake catchments exceeded aquatic demand and may also have had lower Si-isotope values. Since 5.5 ka BP, increasingly dry climates and more open vegetation, reinforced by the spread of agricultural cropland over the last 3–4 ka, have reduced dissolved silica inputs into the lakes. Centennial-to millennial-scale dry episodes are also evident in the isotopic records and merit further investigation.

1. Introduction

The biogeochemical cycles of essential nutrients such as carbon, nitrogen, phosphorus and silicon are major determinants of global climate and ecophysiology on Quaternary time scales (Berner and Berner, 2012; Kump et al., 2013; Schlesinger and Bernhardt, 2013). The Si cycle is interlocked with the carbon cycle (Conley, 2002; Street-Perrott and Barker, 2008) through several key processes: enhancement of silicate rock weathering by biotic activity (Kelly et al., 1998; Lucas, 2001); pumping of dissolved silica (DSi) by higher plants to form biogenic silica (BSi) particles known as opal phytoliths, which are deposited by litterfall and actively recycled by soil processes (Carey and Fulweiler, 2012; Derry et al., 2005; Sommer et al., 2006; Song et al., 2012; Struyf and Conley, 2012); and uptake of DSi by siliceous algae, notably diatoms, in rivers, lakes, reservoirs and oceans (Conley, 1997; De La Rocha and Tréguer, 2012; Frings et al., 2014a; Humborg et al., 2000; Smetacek, 1999). The global DSi flux to the oceans is dominated by large tropical rivers (Gaillardet et al., 1999) and by chemical weathering of basalts (Dessert et al., 2003; Dupré et al., 2003). Since DSi is an essential nutrient for marine diatoms, which largely control the export of organic carbon to the deep ocean (Smetacek, 1999; Yool and Tyrrell, 2003), Quaternary variations in DSi output from tropical rivers could potentially have had a significant impact on the drawdown of atmospheric CO_2 by the marine biological pump.

Major uncertainties still surround the impact of Late Quaternary fluctuations in climate and terrestrial ecosystems on the continental weathering flux of DSi and hence on the oceanic carbon

* Corresponding author.
E-mail address: f.a.street-perrott@swan.ac.uk (F.A. Street-Perrott).

http://dx.doi.org/10.1016/j.quascirev.2015.07.028

cycle (De La Rocha and Tréguer, 2012; De La Rocha and Bickle, 2005; Frings et al., 2014a; Froelich et al., 1992; Laruelle et al., 2009; Lupker et al., 2013; von Blanckenburg et al., 2015). Analyses of Si isotopes in diatomaceous lake muds, which are largely immune to recycling by surface processes, have the potential to elucidate the response of the continental Si cycle to past changes in climate, hydrology, vegetation and chemical weathering (Chen et al., 2012; Street-Perrott et al., 2008; Swann et al., 2010). Here, we reconstruct the response of the Si cycle in the headwaters of the White Nile to variations in climate and human activity since the last major desiccation event (~15 ka BP), using sediment cores from Lakes Victoria and Edward. We employ coupled measurements of Si and O isotopes in diatoms ($\delta^{30}Si_{diatom}$ and $\delta^{18}O_{diatom}$) and lipid biomarkers as tracers for the Si cycle, palaeohydrology and ecosystem changes, respectively. Additional insights are provided by published stratigraphical, geochemical and palaeoecological records from these lakes.

2. Background

2.1. Oxygen isotopes

Studies of O isotopes in diatom silica are relatively well established, for example in temperate latitudes, where it has been shown that the oxygen-isotope values of diatom silica ($\delta^{18}O_{diatom}$), like those of carbonates, are controlled primarily by water temperature and/or by the isotope composition of the lake water (Leng and Barker, 2006; Leng and Marshall, 2004). In the tropics, seasonal temperature changes are small (Rozanski et al., 1996, 1993). Instead, the isotopic composition of lake water is influenced by a combination of factors including the amount of precipitation, the $\delta^{18}O$ value of the water vapour and its trajectory from the source region; although surface processes such as riverine inputs and evaporative enrichment are generally the main controls on $\delta^{18}O_{diatom}$ (Barker et al., 2011, 2007, 2001; Hernández et al., 2011; Hernández et al., 2010; Leng and Barker, 2006; Polissar et al., 2006).

2.2. Silicon isotopes

Processes operating at every stage of the Si cycle can be monitored using the stable isotopes of Si as a tracer (Basile-Doelsch, 2006; Cornelis et al., 2011; De La Rocha, 2002; Ding et al., 1996; Douthitt, 1982). Si has three stable isotopes, ^{28}Si, ^{29}Si and ^{30}Si, which can be measured in silicates and natural waters by mass spectrometry. The $^{30}Si/^{28}Si$ ratio is reported in standard delta notation relative to an international standard (Leng et al., 2009). Si isotopes are not fractionated by the hydrological cycle. However, uptake of DSi to form biogenic silica (BSi) or secondary minerals, which are isotopically depleted, raises the $\delta^{30}Si$ value of the residual solution (Basile-Doelsch, 2006). Hence, the instantaneous $\delta^{30}Si$ value of precipitating silica is dependent on the evolving $\delta^{30}Si$ of the water and the degree of utilization of the available DSi. Theoretically, in a "closed" system such as the oceanic mixed layer or the epilimnion of a large, stratified lake, Si-isotope fractionation by diatoms will follow a Rayleigh model and the $\delta^{30}Si$ of the accumulated silica (recorded by $\delta^{30}Si_{diatom}$ in sediment cores) will rise towards the starting composition of the source water as the DSi supply is exhausted (Alleman et al., 2005; Basile-Doelsch, 2006; De La Rocha, 2006). By contrast, in an open (steady-state) system with a continuous input of nutrients derived from the same external source, $\delta^{30}Si_{diatom}$ values may climb even higher during prolific diatom blooms (Opfergelt et al., 2011; Varela et al., 2004). In the oceans, Si-isotope data have been used as a proxy to reconstruct palaeoproductivity (or more strictly marine silicic-acid use by diatoms relative to initial dissolved silicic-acid concentrations) (Brzezinski et al., 2002; De La Rocha et al., 1998). However, in continental environments, there have been fewer Si-isotope investigations. Si in rivers comprises both dissolved and particulate matter; measurement of both permits assessment of both weathering- and productivity-related fractionation. Modern studies of Si isotopes in large fluvial systems have documented intense biotic Si cycling in the humid tropics (Frings et al., 2014b; Hughes et al., 2012, 2011, 2013), which may progressively elevate $\delta^{30}Si$ values downstream in rivers like the Nile that traverse extensive lakes and wetlands, in which DSi is efficiently stripped from the water by both biotic uptake and neoformation of clays (Cockerton et al., 2013; Ding et al., 2004; Fontorbe et al., 2013).

Modern Si-isotope investigations of lakes have focused on the relationships between climate, hydrogeology, diatom productivity and lake-mixing regimes (Alleman et al., 2005; Opfergelt et al., 2011). These studies, while highlighting the complexity of lake systems (which potentially receive influxes of several weathering-derived components), confirm that Si-isotope ratios are consistent with DSi concentrations (Alleman et al., 2005; De La Rocha et al., 2000; Opfergelt et al., 2011). They also suggest that Si-isotope fractionation by diatoms is independent of species and temperature, offering potential information on past changes in nutrient supply and diatom production. However, few previous studies have analysed Si isotopes in biogenic components of Quaternary lake sediments (Chen et al., 2012; Stephens, 2011; Street-Perrott et al., 2008; Swann et al., 2010). For this reason, we compare our Si-isotope data in this paper with new measurements of lipid biomarkers and published palaeoenvironmental data in order to validate our interpretations.

2.3. Lipid biomarkers

The organic fraction of lacustrine sediments comprises a mixture of autochthonous compounds synthesized by living organisms that lived within the lake, such as algae, bacteria and submerged/floating macrophytes, and allochthonous inputs from the catchment, notably from vascular land plants. *n*-Alkanes, which are least susceptible to degradation, are most commonly used in palaeoenvironmental reconstructions (Meyers, 1997; Meyers and Ishiwatari, 1993). Suites of *n*-alkanes characteristic of certain plant groups can be used to investigate contributions from specific sources (i.e. terrestrial *vs.* aquatic). Odd-numbered, long-chain homologues (C_{27}–C_{35}) are generally characteristic of terrestrial higher-plant leaf waxes (Eglinton and Hamilton, 1967), whereas short-chain homologues (C_{17}–C_{21}) are characteristic of aquatic algae (Cranwell et al., 1987) but vulnerable to diagenesis. Ficken et al. (2000) demonstrated that mid-chain-length (C_{23}–C_{25}) *n*-alkanes formed the main component of leaf waxes produced by submerged and floating (non-emergent) aquatic macrophytes.

Biomarker ratios of long- and mid-chain *n*-alkanes are used here to assess the relative contributions from vascular-plant sources. The P_{wax} ratio is given by the abundance of long-chain *n*-alkanes over the sum of mid- and long-chain *n*-alkanes ($P_{wax} = (C_{27} + C_{29} + C_{31})/(C_{23} + C_{25} + C_{27} + C_{29} + C_{31})$), and reflects the proportions of leaf waxes derived from terrestrial plants and emergent aquatic macrophytes such as reeds, relative to those derived from submerged/floating aquatic macrophytes (Zheng et al., 2007). Ficken et al. (2000) proposed the *n*-alkane P_{aq} proxy ($P_{aq} = (C_{23} + C_{25})/(C_{23} + C_{25} + C_{29} + C_{31})$) to distinguish the relative contribution of submerged/floating aquatic macrophytes from that of emergent aquatics and terrestrial plants. A P_{aq} value of >0.4 signifies that an important fraction of the *n*-alkanes originated from submerged/floating plants (Ficken et al., 2000).

Odd-numbered, mid-to long-chain *n*-alkenes in lake sediments are widely used as algal indicators (de Mesmay et al., 2007;

Matsumoto et al., 1990; Theissen et al., 2005; Xu and Jaffé, 2009; Zhang et al., 2004). Reported sources for these compounds have rather diverse ecologies and include cyanobacteria, green (e.g. *Scenedesmus*, *Botryococcus braunii*) and yellow–green (eustigmatophyte) algae (e.g. *Nannochloropsis*) (Xu and Jaffé, 2009). Zhang et al. (2004) formulated a proxy for algal inputs based on the proportion of *n*-alkenes plus a hydrocarbon compound produced by *B. braunii* (cyclobotryococcatriene), relative to terrestrial-plant leaf waxes. $P_{alg} = (C_{23:1} + C_{25:1} + C_{27:1} + \text{cyclobotryococcatriene})/(C_{23:1} + C_{25:1} + C_{27:1} + \text{cyclobotryococcatriene} + C_{29} + C_{31} + C_{33})$. However, cyclobotryococcatriene was not identified in Lake Victoria or Lake Edward sediments, so the P_{alg} formula was revised for this paper: $P_{alg} = (C_{23:1} + C_{25:1} + C_{27:1})/(C_{23:1} + C_{25:1} + C_{27:1} + C_{29} + C_{31} + C_{33})$.

3. Regional setting

3.1. Lake Victoria

Lake Victoria (68,800 km^2) is the third largest lake in the world (Kendall, 1969) and straddles the Equator between the eastern and western branches of the East African Rift System (Fig. 1). It is located at 1134 m a.s.l in the headwaters of the White Nile. It is relatively shallow with a mean depth of 40 m and a maximum depth of 68 m (Johnson et al., 2000). The catchment directly surrounding the lake is relatively flat, not exceeding ~25 m above the lake surface (Kendall, 1969), whereas the outer drainage basin to the east and west is enclosed by the shoulders of the rift valleys, with elevations exceeding 2000 m a.s.l. (Fig. 1).

Lake Victoria is an "open, atmosphere-controlled" lake with a large area:volume ratio (Spigel and Coulter, 1996; Street-Perrott and Harrison, 1985), which makes its water balance and lake level moderately sensitive to climate change, especially when the latter drops below its outflow to the White Nile (Street-Perrott, 1995). It probably desiccated at least twice during the Last Glacial Maximum (LGM), as identified by seismic reflectors and palaeosols in deep-water cores (Johnson et al., 1996; Kendall, 1969; Stager et al., 2002; Talbot and Lærdal, 2000). This study focusses mainly on the time interval since the last desiccation event, which ended ~15 ka BP ago (Berke et al., 2012).

The Lake Victoria catchment is largely underlain by Precambrian granitic and metamorphic rocks. Small pockets of Cenozoic volcanics are found on its eastern and western borders (Schlüter, 2008). Intense leaching of mobile cations and Si under the hot, humid, interglacial climate of the rift flanks has led to widespread development of deep, ferralitic soil profiles. Fluvial sediments draining these areas are dominated by relatively inert weathering residues (quartz sand and kaolinite clays) (Garzanti et al., 2013a, 2013b). These conditions are typical of a transport-limited chemical-denudation regime (Stallard, 1995; Street-Perrott and Barker,

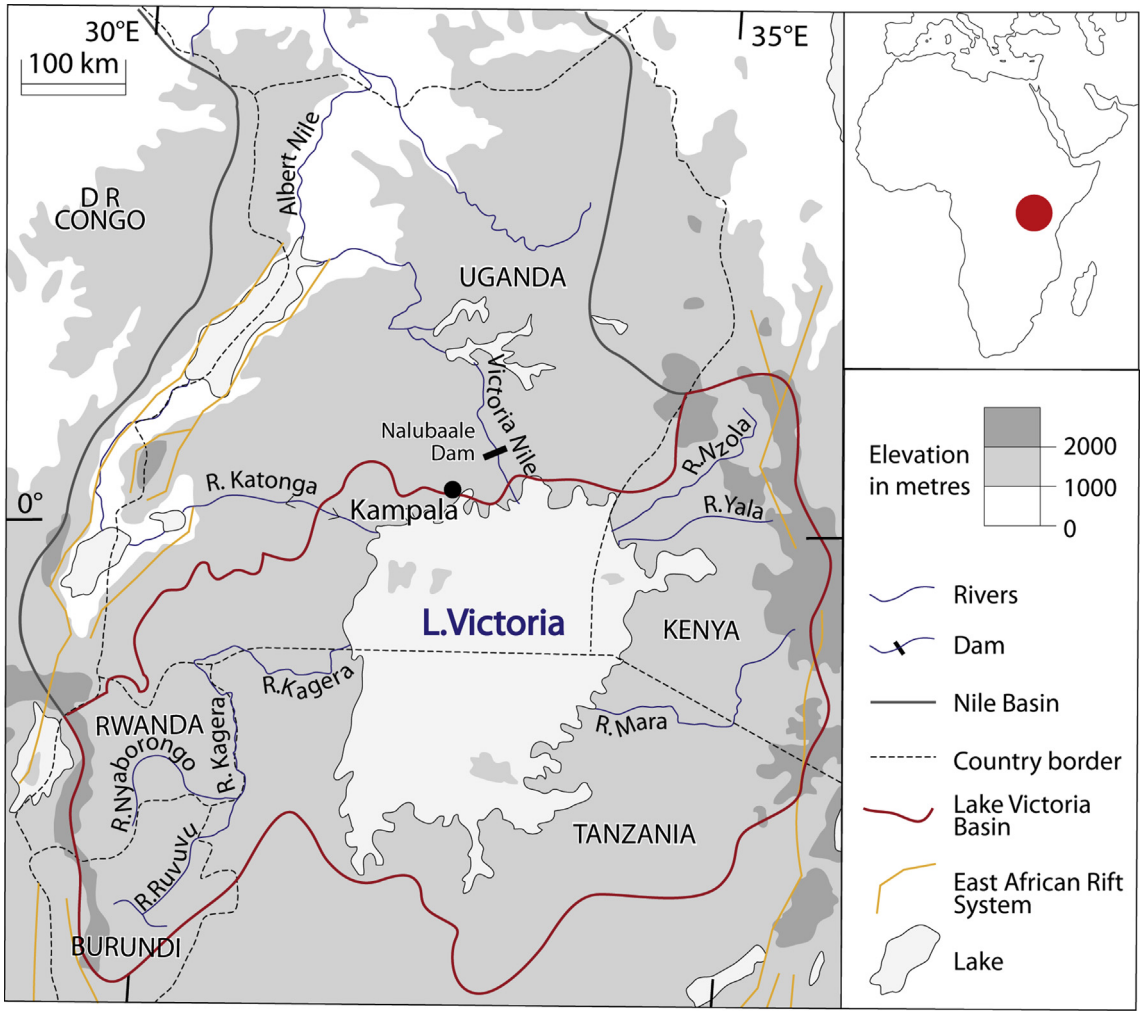

Fig. 1. Location map of Lake Victoria.

2008).

The Lake Victoria Basin experiences a bimodal rainfall distribution with "long rains" occurring between March and May and "short rains" between October and December. Annual precipitation is ~1250–1500 mm/yr in the plains surrounding the lake and >2000 mm/yr in the highlands. The annual variation in rainfall is largely governed by the north–south migration of the Inter-tropical Convergence Zone (ITCZ), where the north-east and south-east monsoons meet (Johnson et al., 2000). To the west, the Congo Air Boundary (CAB) separates moist, Atlantic airflows from south-east tradewinds sourced from the Indian Ocean (Nicholson, 1996; Tierney et al., 2011). Rainfall distribution is also influenced by the lake itself; its large area and circular geometry promote strong land–lake circulations (Flohn and Fraedrich, 1966). ~85% of water inputs originate from rain falling directly onto the lake surface (Sutcliffe, 2009; Sutcliffe and Parks, 1999). Mean annual air temperatures around Lake Victoria range from 16–17 °C (min.) to 27–30 °C (max.), and in the highlands from 22–24 °C to <10 °C (Hughes and Hughes, 1992). Evaporation rates are high, particularly over the lake surface, from which ~90% of water losses take place (Nicholson, 1998; Piper et al., 1986; Sutcliffe, 2009; Sutcliffe and Parks, 1999). Elevated modern lake-water $\delta^{18}O$ values (Cockerton et al., 2013) suggest that evaporation exerts a strong influence over O isotopes, enhancing their sensitivity to shifts in climate.

The lake catchment covers 194,000 km^2 (Piper et al., 1986) (Fig. 1). The Kagera River, draining the highlands of Burundi and Rwanda, is the principal inflow. The Katonga River and several small tributaries in the north-east of the basin constitute the remainder of the major surface inputs (Sutcliffe and Parks, 1999). The only outflow occurs at Jinja at the north end of the lake *via* the Victoria Nile, marking the beginning of the White Nile, to which it provides a steady base flow throughout the year. Lake Victoria is monomictic; overturn of the water column occurs during the cooler, windier season in May–August when strong southerly winds cause upwelling of nutrients.

Modern terrestrial vegetation in the lowlands (<2000 m) of the Lake Victoria Basin is predominantly woodland and savanna (Langdale-Brown et al., 1964; White, 1983). Enhanced rainfall in the northern and western parts of the basin supports pockets of lowland rainforest and on the highland peripheries, montane rainforest. Large areas are cultivated for subsidence farming (e.g. plantains, cassava, sweet potatoes and bananas) or used for grazing, creating a mosaic of natural vegetation and cultivated crops. The lake fringes and the floodplains of its tributaries are characterised by wetlands, supporting a variety of submerged and emergent macrophytes. In the lower reaches of the Kagera River, a 150 km-long stretch is flanked by a zone of lakes and swamps up to 15 km wide and dominated by *Cyperus papyrus* (C_4 emergent sedge) and *Vossia cuspidata* (C_4 aquatic grass) (Sutcliffe and Parks, 1999). The lake itself is surrounded by extensive swamps with *C. papyrus* and *Miscanthidium violaceum* (C_4 aquatic grass).

3.2. Lake Edward

Lake Edward occupies a half-graben at an altitude of 912 m a.s.l. in the Western Rift (Fig. 2). It has a surface area of 2325 km^2 and a maximum depth of 117 m (Lærdal and Talbot, 2002; Russell et al., 2003a). The lake is bounded to the north by the Rwenzori Mountains (>5000 m), to the west by the steep rift escarpment (2500–3000 m a.s.l.), to the south by the Virunga Volcanoes (>4500 m a.s.l.) and to the east by the more gently rising Kigezi Highlands (1500–2700 m a.s.l.).

The northern part of the Western Rift system is largely underlain by Precambrian basement rocks (gneisses and granites), with areas of Quaternary alluvial deposits around the Great Lakes and their associated river valleys. Neogene volcanics (notably alkali basalts) can be found in the Virunga Mountains and in small volcanic craters and vents close to Lakes George and Edward (Schlüter, 2008). A north–south fault scarp, the Kasindi Fault Zone (KFZ), divides Lake Edward into two sub-basins and has significantly affected sedimentation patterns. The deepest point lies to the west of the KFZ, with the shallower eastern basin being subject to small-scale faulting (Lærdal and Talbot, 2002; Lærdal et al., 2002; Russell et al., 2003a).

Like Lake Victoria, the Lake Edward Basin exhibits a bimodal rainfall regime with rainy seasons from October to December and March to May in association with the twice-yearly passage of the ITCZ (Nicholson, 1996). Lake Edward also receives moisture from the south-easterly Indian Ocean monsoon, though its close proximity to the CAB suggests that a substantial contribution originates from the Atlantic Ocean *via* the Congo Airstream (Russell and Johnson, 2006). Annual rainfall is about 900 mm/yr over the lake with substantially greater amounts falling at higher elevations (Viner and Smith, 1973).

The catchment of Lake Edward covers 15,840 km^2. The lake is fed primarily by rivers draining the surrounding mountains (Fig. 2) (Lehman, 2002; Russell and Johnson, 2006). These areas of steep relief are probably subject to a weathering-limited chemical-denudation regime (Stallard, 1995; Street-Perrott and Barker, 2008). In addition, the Kazinga Channel, a 30 km-long, 1 km-wide, drowned river valley that flows sluggishly from the shallow, hypereutrophic Lake George (914 m a.s.l.) to the east, is a major inflow. Lake George is mainly fed by streams draining the Rwenzori Mountains (Russell and Johnson, 2006). Its large population of hippos (*Hippopotamus amphibius*), which graze on land and defecate in the water, probably adds substantial amounts of partially digested BSi to the lake and the Kazinga Channel (J. Schoelynck, pers. comm. 2015). Currently, Lake Edward overflows into the Semliki River, which runs northwards into Lake Albert and thence to the White Nile. Unfortunately, gauging stations are sparse, although river runoff is believed to be its most important source of water (Lehman, 2002). Russell and Johnson (2006) calculated from isotopic data that 54% of water losses occur through evaporation and the remainder through the outflow. Together, these estimates suggest that Lake Edward should be classified as an "open, reservoir lake", with a modern water balance governed by riverine inflows and outflows, which implies that it was most sensitive to long-term climate change during periods when its water level dropped below the outlet, especially if there was a pronounced decrease in riverine inputs (Street-Perrott, 1995; Street-Perrott and Harrison, 1985), for example due to desiccation of Lake George. Lake Edward is permanently anoxic below 30 m water depth but only weakly thermally stratified; it is currently mesotrophic (Russell and Werne, 2009).

Vegetation in the Rift Valley floor surrounding Lake Edward consists of a mosaic of evergreen bushland and thicket, secondary *Acacia* wooded grassland and farmland. In the highlands east of Lake Edward and northeast of Lake George, forest reserves protect large remnants of moist semi-deciduous rainforest while in the mountains to the north, west and south, Afromontane rainforest grades upwards into Ericaceous shrubland and then Afroalpine vegetation (Beuning and Russell, 2004; Jolly et al., 1997; Langdale-Brown et al., 1964; Livingstone, 1967; White, 1983). The contrast in vegetation between the plains and the higher ground is attributable to the rainshadow effect of the surrounding mountains. Large areas of graminoid wetland dominated by *C. papyrus* or *Phragmites mauritianus* (C_3 grass) occupy the mouths of tributaries entering Lake Edward (Hughes and Hughes, 1992) and surround Lake George (Green, 2009; Hughes and Hughes, 1992). Extensive wetlands also exist in some headwater regions, particularly the Kigezi Highlands

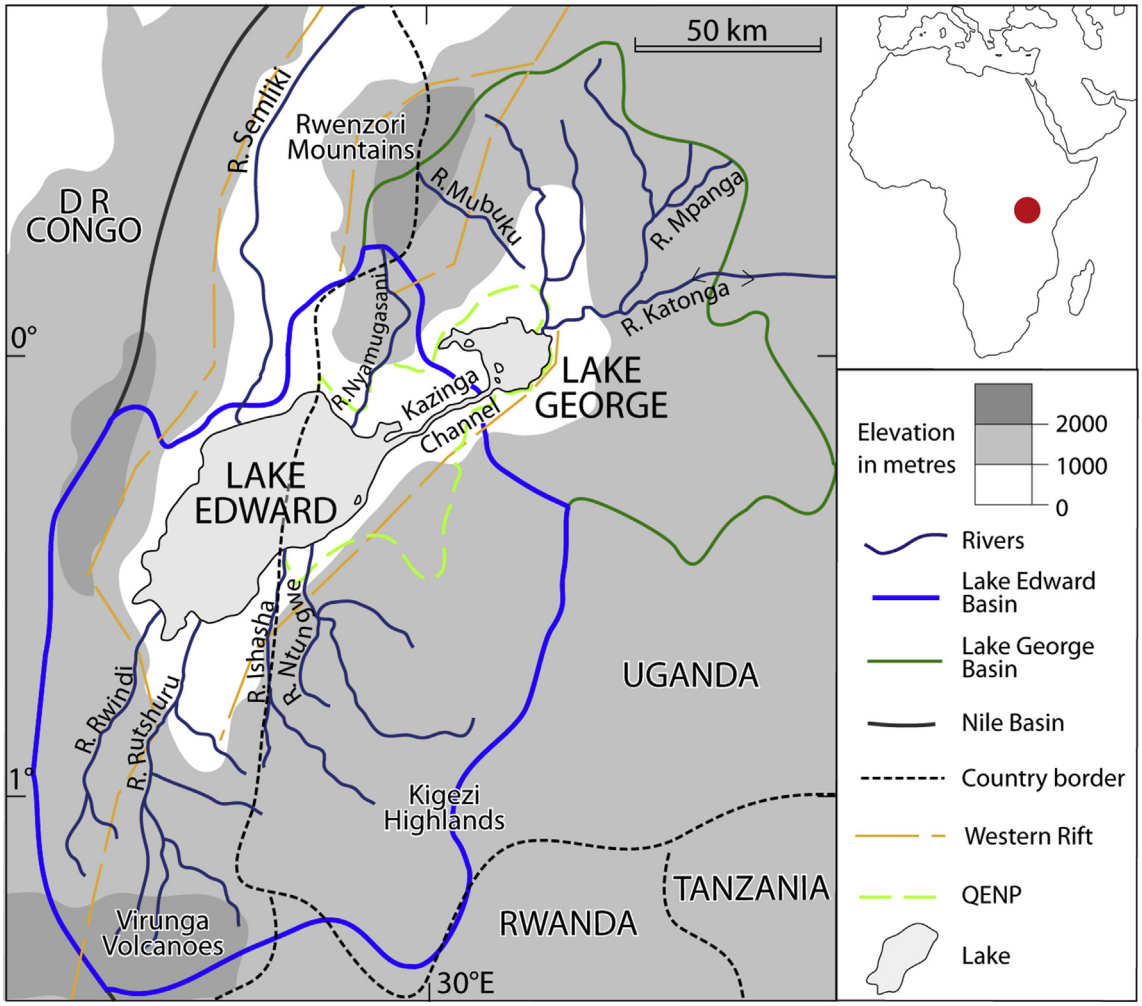

Fig. 2. Location map of Lake Edward.

(Green, 2009). In Lake Edward, *Potamogeton pectinatus* is the dominant submerged macrophyte, together with *Najas marina* and *Vallisneria aethiopica* (Hughes and Hughes, 1992).

4. Previous palaeolimnological investigations

4.1. Lake Victoria

Prior to 1995, only five long sediment cores were collected from Lake Victoria and analysed for pollen, diatoms and bulk organic geochemistry (Kendall, 1969; Stager, 1984; Stager et al., 1997, 1986; Talbot and Livingstone, 1989). All these cores were obtained from the northern part of the lake close to the current shoreline and thus may not represent basin-wide conditions (Johnson, 1996). In 1995 and 1996, nine additional cores of varying length and basal age were recovered by the International Decade for East Africa Lakes (IDEAL) multidisciplinary project. Offshore coring sites were selected based on seismic-reflection profiles in order to obtain long, continuous records spanning the Late Pleistocene and Holocene. The IDEAL cores are curated by the US National Lacustrine Core (LacCore) Facility at the Limnological Research Center, University of Minnesota.

During the LGM, a double vertisolic palaeosol in multiple sediment cores shows that Lake Victoria desiccated at least twice; the ^{14}C chronology of these events is still debated, but one or other may correspond to the intensely cold/dry Heinrich event H-1 of higher latitudes (Johnson et al., 1996; Stager and Johnson, 2008; Stager et al., 2011; Talbot and Lærdal, 2000). Based on the TEX_{86} index, water temperatures were at least 6 °C cooler at ~15.2 ka BP but rose rapidly as the lake started to refill (Berke et al., 2012; Stager and Johnson, 2008). Lake Victoria overflowed into the White Nile from ~14.2 to 14 ka BP onwards (Talbot et al., 2000; Williams et al., 2006). A short period of lower water level just prior to ~11.5 ka BP has been correlated with the cold/dry European Younger Dryas event (Johnson et al., 2000; Kendall, 1969; Williams et al., 2000).

Tropical aridity and weakening of the African monsoon rains during the LGM, culminating in complete desiccation of Lake Victoria, have been attributed to complex interactions between orbital geometry, atmospheric composition, ocean circulation and land-surface conditions (Gasse, 2000; Gasse et al., 2008; Kiage and Liu, 2006; Stager et al., 2002). Increasing June–July–August (JJA) insolation amplified the boreal summer monsoon during the African Humid Period (AHP) between ~15 and 5.5 ka BP, creating wetter and warmer conditions across northern and equatorial Africa (Barker et al., 2004; deMenocal et al., 2000; Gasse, 2000; Kutzbach and Street-Perrott, 1985), resulting in abrupt filling of Lake Victoria and the onset of overflow into the Victoria Nile. Superimposed on these long-term climatic trends were millennial-scale events associated with major atmosphere–ocean reorganizations, notably Heinrich event H-1 and the Younger Dryas (Bard et al., 2000; Bond et al., 1992; Street-Perrott and Perrott, 1990), providing a link between major climatic events in the tropics and the high latitudes (Stager et al., 2002, 2011).

A shift from savanna grasses during the LGM to semi-deciduous forest took place ~14 ka BP, shortly after the refilling of Lake Victoria (Kendall, 1969). At the beginning of the Holocene, the development of moist evergreen forest indicated increased humidity and rainfall, following a brief increase in grass pollen during the Younger Dryas event.

Diatom palaeoecological studies highlight the nearly synchronous changes in lacustrine and terrestrial environments within the Lake Victoria basin (Stager et al., 2003; Stager and Johnson, 2000; Stager et al., 1986). Diatom assemblages above the upper palaeosol represent rising water levels, although the lake water was initially chemically concentrated (Kendall, 1969; Stager and Johnson, 2000). High total organic carbon (TOC) and hydrogen-index (HI) values indicate an increasing contribution from phytoplankton, providing evidence for deepening water in a transgressive basin (Talbot and Lærdal, 2000). During the cooler Younger Dryas interval (~13–11.5 ka BP), the water level temporarily dropped and outflow may have ceased in response to renewed aridity (Berke et al., 2012; Johnson et al., 2000; Stager et al., 1997; Stager and Johnson, 2000).

High diatom productivity at the start of the Holocene, implied by elevated BSi concentrations (Johnson et al., 1998), was associated with maximum precipitation/evaporation (P/E) ratios and thorough water-column mixing under windy conditions (Stager et al., 1997, 2003; Stager and Johnson, 2000). An abrupt 8‰ lowering of $\delta^{18}O$ in aquatic cellulose, accompanied by a 23‰ decrease of δD in terrestrial leaf waxes (C_{28} fatty acid), confirms the strong positive trend in water balance (Berke et al., 2012; Beuning et al., 2002). However, between ~9.8 and 7.5 ka BP diatom productivity rapidly declined, as shown by low BSi concentrations in several of the IDEAL cores (Johnson et al., 2000). Johnson et al. (1998) used a mass-balance model to estimate that silica cycling in Lake Victoria would only be able to sustain itself for ~40 years by utilizing its internal reservoir of DSi. Hence, the long-term supply of Si to the lake ecosystem must have been controlled by inputs from the catchment (Johnson et al., 1998), as is the case for other large tropical African lakes such as Malawi and Edward (Bootsma, 2003; Johnson et al., 2001, 2002; Russell and Johnson, 2005).

The reduction in duration and/or intensity of wind-driven mixing continued into the mid-Holocene (Johnson et al., 2000; Kendall, 1969; Stager et al., 1997, 2003; Stager and Johnson, 2000; Talbot and Lærdal, 2000). A transition from evergreen to semi-deciduous forest after ~6.8 ka BP marks the development of more pronounced dry seasons (Kendall, 1969; Stager et al., 1997, 2003). By ~5 ka BP, declining diatom abundance and a shift to pennate diatoms indicate lower water levels with more extensive shallows (Stager, 1984; Stager and Johnson, 2000). A further reduction in water-column mixing was inferred from the presence of *Nitzschia fonticola* (Stager et al., 1997, 2003; Stager and Johnson, 2000). Forest decline starting at ~3.2 ka BP may reflect the penetration of agriculture into East Africa (Kendall, 1969), while an accompanying rise in sedge and grass pollen suggests encroachment of swamp vegetation at inshore sites and expansion of regional grasslands.

IDEAL core V95-1P (00° 27.63′S, 33° 24.09′E) was selected for this study due to its long and continuous record dating back to ~21 ka BP (Berke et al., 2012; Johnson et al., 2000) and to the availability of core material. This core was collected from a water depth of 68 m in the north-eastern part of the lake. It has a total length of 906.5 cm. Two palaeosols are present at 906.5–741.5 and 686–619.5 cm, separated by a ~55 cm-thick, fine grained mud with large plant macrofossils including reed-stem fragments. Above 619.5 cm, a gradual transition into homogenous, massive, lacustrine muds marks the late-glacial transgression. These muds constitute the remainder of the core, becoming diatomaceous between ~550 and 400 cm.

4.2. Lake Edward

Apart from initial investigations in the 1970s (Hecky and Degens, 1973), little work was carried out on the palaeolimnology of Lake Edward before the IDEAL expedition in 1996. A total of four IDEAL cores of varying length and age was collected; between them these span the Holocene epoch. Their sediment stratigraphy and radiocarbon ages provide evidence of reworked sediments and prolonged hiatuses, particularly in the shallower cores (Beuning and Russell, 2004; Lærdal et al., 2002; Russell et al., 2003a). In addition to climate change, rift tectonics have caused lake-level changes and slumping of older deposits, making it difficult to separate these two influences in some cases (Lærdal et al., 2002). An insight into climatic conditions during the LGM is provided by a slump deposit within the Holocene muds of core E96-2P, dated to 20,600 ^{14}C yr BP (Lærdal et al., 2002; Russell et al., 2003a). Its lithological properties and geochemical composition suggest precipitation of high-Mg endogenic calcite from highly evaporated lake waters, indicating a more arid climate (Beuning and Russell, 2004; Lærdal et al., 2002; Russell et al., 2003a).

The continuous palaeoclimatic record from Lake Edward comprises an early-to mid-Holocene interval of high lake levels resulting from an orbitally forced increase in monsoon rainfall, followed by increasing aridity from ~5.2 ka BP onwards, as the duration or intensity of the rainy seasons declined (Russell and Johnson, 2005; Russell et al., 2003a, 2003b). Superimposed on this long-term evolution, several centennial-to millennial-scale events have been identified, particularly at ~4 and 2 ka BP (Russell and Johnson, 2005). Late Holocene climatic events of multi-decadal duration (Russell and Johnson, 2005, 2007; Russell et al., 2003a, 2003b) are not discussed here since the main focus is on orbital-scale changes.

Evidence for wet conditions during the early-to mid-Holocene (~11.2–6.7 ka BP) comes largely from pollen evidence showing that moist semi-deciduous, lowland–forest taxa predominated. Lake levels as much as 12.5 m higher than today were reconstructed from shorelines dated 11.2–9 ka BP by Beuning and Russell (2004). During this period, Lake Edward was periodically and perhaps seasonally mixed (Russell et al., 2003a). An observed decline in lake level from 9 to 5.2 ka was attributed to tectonic lowering of the Semliki outlet rather than to climate change (Lærdal et al., 2002; Russell et al., 2003a). Beuning and Russell (2004) estimated that an increase of 25–60% in annual precipitation compared to present (1500–2000 *vs.* 1200 mm/yr today) would be required to sustain extensive moist, semi-deciduous forest on the Rift floor. Maximum wetness between ~9 and 6.7 ka BP was inferred from slight changes in pollen assemblages, relatively high sedimentary S concentrations (a tracer for Fe delivery from the catchment) and clastic sedimentation indicative of increased runoff. Several poorly dated, millennial-scale oscillations in stratification occurred between 9 and 5.2 ka (Russell et al., 2003a).

BSi concentrations declined gradually during the early to mid-Holocene, suggesting to Beuning and Russell (2004) that increased flow though the outlet due to an increase in P/E resulted in a decreased residence time of DSi in the lake. In contrast, Russell and Johnson (2005) argued that increased wetness would have mobilised more DSi, resulting in an increased rate of BSi accumulation if diatoms had dominated the phytoplankton. As with Lake Victoria and some of the other large African lakes such as Malawi (Bootsma, 2003), the DSi stock in the hypolimnion of Lake Edward is too small to sustain the long-term changes seen in the BSi record. Russell and Johnson (2005) calculated that the residence time of DSi in Lake Edward is only ~4 yr and concluded that riverine inputs to the lake controlled long-term changes in the supply of DSi.

The onset of drier conditions at ~5.2 ka BP at Lake Edward was

marked by the start of endogenic calcite precipitation. A long-term rise in the Mg content of calcite suggested a progressive increase in evaporative concentration (Kelts and Hsü, 1978; Russell and Johnson, 2005; Russell et al., 2003a). Ferruginous sands in core E96-2P provided evidence of lake low stands between ~4.4 and 2.0 ka BP (Russell et al., 2003a). A drought event identified at ~4.2 ka BP (Russell and Johnson, 2005; Russell et al., 2003b) coincided with a severe drying episode recognised in many other East African palaeoclimate records (Gasse, 2000; Street-Perrott and Perrott, 1993). Lake George desiccated and the level of Lake Albert fell (Beuning et al., 1997; Viner, 1977), suggesting regional aridity in western Uganda. A more significant low stand of Lake Edward at ~2 ka BP is marked by a 7% increase in mole% Mg in calcite (Russell and Johnson, 2005; Russell et al., 2003b). Desiccation of Lake George would have resulted in abrupt cessation of the warm, nutrient-rich inflow through the Kazinga Channel (Russell et al., 2003a). The level of Lake Edward rose shortly after ~2 ka BP, possibly indicating re-establishment of inflow from Lake George (Russell et al., 2003a). From ~2 ka BP onwards, a slight decrease in mole% Mg suggests a return to wetter conditions. The $\delta^{18}O$ values of calcite confirmed these long-term trends (Russell and Johnson, 2005; Russell et al., 2003b).

Samples from three of the four cores obtained during the IDEAL expedition (E96-1P, E96-5M and E96-2P, hereafter referred to as 1P, 5M and 2P) were used in this study to form a composite sequence of Holocene pelagic muds and diatomaceous oozes, in order to avoid the shell concentrates, sand units, slumps and hiatuses found in individual cores (Beuning and Russell, 2004; Lærdal et al., 2002; Russell et al., 2003a; Russell and Kelts, 1999). Core 1P (0°15.5′S, 29°35.0′E), with a length of 706 cm, was collected from 63 m water depth in the western basin, the deepest site to be cored. Core 5M (0°21.4′S, 29°42.1′E) was the longest (768.5 cm), obtained from 30 m water depth to the east of the KFZ. Core 2P (0°18.9′S, 29°37.1′E) was 489 cm long and was collected from 46 m depth in the western basin. Full stratigraphical descriptions are given by Russell et al. (2003a) and Beuning and Russell (2004).

5. Materials and methods

5.1. Core sampling

Archived sediment samples from the Lake Victoria and Edward cores were supplied by the LacCore Facility. In order to focus on broad glacial/interglacial changes, the cores were generally sampled at ~500 yr resolution back to the period of lowest lake levels at the end of the last glacial (~21 ka), or as far back as individual cores allowed. This period spans the arid conditions at the end of the LGM, the onset of the AHP at ~15 ka BP and the shift to drier conditions from ~5.5 ka BP to present. Beneficially, many of the cores had already had their biogenic silica (BSi) content and/or diatom concentrations determined, which aided the selection of samples for isotopic analysis.

To isolate enough diatoms for isotopic analysis (~5 mg) (Leng and Sloane, 2008), the initial BSi concentrations needed to be relatively high (~10%). If the diatom concentration was lower, a correspondingly larger amount of sediment was processed. Prior work on the sediments of Lakes Victoria and Edward provided confidence in their suitability for extracting pure diatom components, since their BSi concentrations peak at >35% (Johnson et al., 2000; Russell et al., 2003a).

5.2. Diatom extraction

Several chemical and physical methodologies have been suggested for isolating and cleaning diatom frustules (Leng and Barker, 2006). The methods used here to remove contaminants were tailored specifically to each individual sample, depending on its composition. The first step used HCl to remove carbonates, followed by H_2O_2 to remove organics (Morley et al., 2004). An additional step with concentrated HNO_3 was employed to remove resistant organic matter and to etch the surface of the diatom frustules to release any clays trapped within the pores. The samples were then sieved at 63, 38 and 20 μm using deionised water. This step allowed samples to be divided and isolated into “groups” of contaminants, for example silts and clays, for ease of determining the next suitable methodological step and to concentrate the diatoms. Subsequently differential settling, heavy liquid separation using sodium polytungstate, sonication and SPLITT (gravitational split-flow thin fractionation) were used to varying degrees (Leng and Barker, 2006) before the split samples were recombined. Assessment of the degree of purity of the samples was done visually under a light microscope and a Scanning Electron Microscope (Fig. 3). The resultant pure diatom fractions were dominated by planktonic forms yet remained taxonomically mixed, as it was impossible to separate a single species. However, evidence for vital effects that exceed analytical error is limited (Brandriss et al., 1998; Moschen et al., 2005; Schiff et al., 2009; Shemesh et al., 1995).

5.3. Diatom isotopes (^{18}O, ^{30}Si)

For the O- and Si-isotope analyses of diatom silica (Leng and Sloane, 2008), pure diatom samples were analysed at the NERC

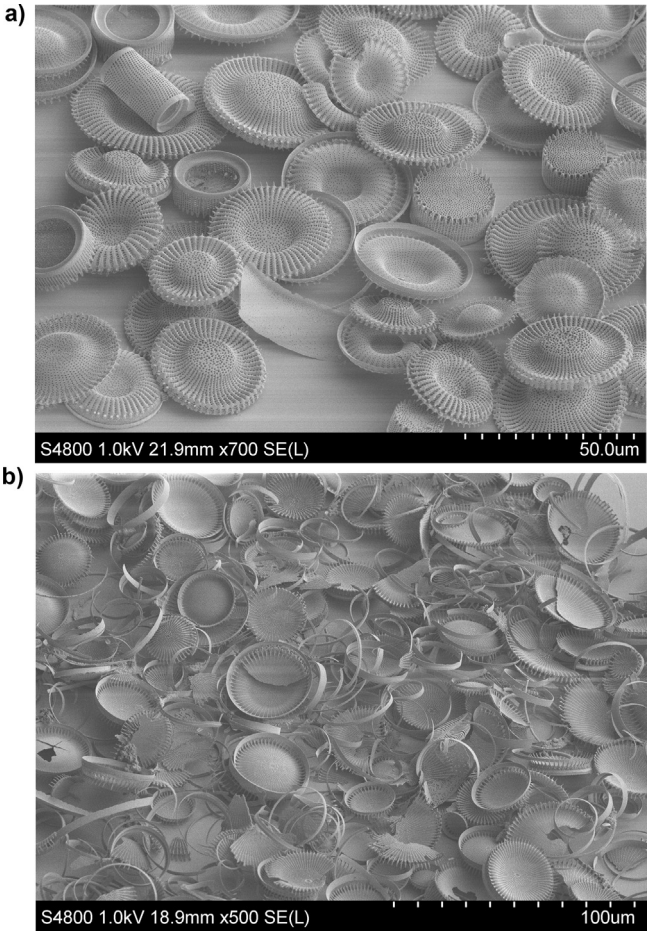

Fig. 3. SEM photomicrographs of cleaned samples of planktonic diatoms: a) from Lake Victoria, dominated by *Stephanodiscus* and *Aulacoseira* spp; and b) from Lake Edward, dominated by *Stephanodiscus* spp.

Isotope Geosciences Facilities, British Geological Survey, using a step-wise fluorination technique. 3–5 mg of purified diatoms were loaded into Ni reaction tubes where they were outgassed for 2 h at 250 °C to remove surficial water. Reaction with BrF_5 at 250 °C for 6 min removed the outer layer of diatom silica (hydrous layer) containing exchangeable oxygen, before a full reaction with an excess of reagent at 500 °C for 14 h to dissociate the silica into oxygen, which was subsequently converted into CO_2, and silicon to SiF_4, following the method described by Clayton and Mayeda (1963). After extraction, the collected gases were analysed for O and Si isotopes using a Finnigan MAT™ 253 Isotope Ratio-Mass Spectrometer. Full details of the fluorination line and methodology are given by Leng and Sloane (2008). All $\delta^{18}O$ and $\delta^{30}Si$ data are reported relative to VSMOW and NBS-28, respectively, using the NIGL within-run laboratory standard (BFC diatomite). Accuracy (2σ) was checked on reference material BFC ($\delta^{18}O$: +28.88 ± 0.36‰, n = 13; $\delta^{30}Si$: +0.05 ± 0.15‰, n = 7), which yielded isotope compositions indistinguishable from previously published values (Chapligin et al., 2011; Leng and Sloane, 2008). Replicate analyses of sample material indicated a mean analytical reproducibility (1σ) of 0.19‰ (range: +0.08 to +0.30‰, n = 6) and 0.07‰ (range: +0.01 to +0.19‰, n = 8) for $\delta^{18}O_{diatom}$ and $\delta^{30}Si_{diatom}$, respectively. Quality control of mass bias was checked by plotting $\delta^{29}Si$ against $\delta^{30}Si$.

5.4. Lipid biomarkers

Sediments from Lakes Victoria and Edward were sampled at ~500-year resolution for total lipids (n = 59). A known amount of freeze-dried, ground sediment (~1 g) from each depth was extracted with dichloromethane (DCM)/methanol (9:1 v/v) using an accelerated solvent extractor (Dionex: ASE 200) at 100 °C and 1500 psi for 25 min in 1 cycle. Following the methods of Ficken et al. (1998) and Huang et al. (1999), total extracts were split into acid and neutral fractions using solid-phase extraction (Aminopropyl Bond Elut® cartridges). The neutral fraction was eluted with DCM/isopropanol (2:1 v/v) and the acid fraction recovered using 2% acetic acid in ether. The neutral fraction was fractionated further into a hydrocarbon and a polar fraction by column chromatography using freshly activated alumina, eluting the hydrocarbons with hexane/DCM (9:1 v/v) and subsequently the polar fraction with methanol/DCM (1:1 v/v). The acid and polar fractions are not discussed here. The hydrocarbon fraction was de-sulphurized by the addition of activated Cu turnings prior to the separation of the branched hydrocarbons (non-adduct fraction) from the straight-chain hydrocarbons (adduct fraction) by urea adduction. A known amount of standard solution (*n*-C_{36} alkane) was added to each sample prior to analysis by gas chromatography–mass spectrometry (GC–MS).

Quantification and identification of straight-chain hydrocarbons (adduct fraction: *n*-alkanes and *n*-alkenes) and branched hydrocarbons (e.g. botryococcenes) were carried out by GC–MS performed on an Agilent 6890 gas chromatograph (split/splitless injection, 70 eV, EI) interfaced directly with an Agilent 5975 mass spectrometer. A HP5-MS fused silica capillary column (30 m × 0.25 mm; 0.25 μm film thickness) was used. The oven temperature was held at 60 °C for 1 min, ramped at 10 °C per minute to 180 °C and then ramped at 4 °C per minute to 300 °C where it was held for 15 min. He was used as the carrier gas.

5.5. Chronology

Existing radiocarbon age models for Lakes Victoria and Edward (Beuning and Russell, 2004; Johnson et al., 2000; Russell et al., 2003a) were used in order to permit direct comparisons with published data. These employed linear interpolation between dates to allow for varying sedimentation rates. However, all radiocarbon dates have been re-calibrated here using CALIB version 6.0 (Stuiver et al., 2012).

6. Results

6.1. Lake Victoria

Diatoms dominated the BSi fraction of Lake Victoria sediments (>99%) apart from the occasional sponge spicule or phytolith. The size fraction most commonly used for isotope analysis was the 20–38 μm fraction, composed predominantly of planktonic *Stephanodiscus* and *Aulacoseira* spp. with occasional fragments of large *Surirella* spp. Breakage of diatom frustules may have occurred during cleaning for isotope analysis, as the remainder of the diatoms were well preserved throughout the core and there were no signs of dissolution or diagenesis (Fig. 3). Only samples at least 97% free from contamination were used for isotope measurements (n = 10). None of the material analysed showed evidence of contamination based on replicate analyses and the observed mass-dependent relationship between $\delta^{29}Si$ and $\delta^{30}Si$.

In the sediments analysed (dated ~14.9–1.4 ka BP), $\delta^{18}O_{diatom}$ values varied over a fairly narrow range (4.6‰), from +39.4 to +44.0‰ (Fig. 4). During the late-glacial transgression, as the level of Lake Victoria rose, $\delta^{18}O_{diatom}$ decreased from +43.5‰ at ~14.9 ka BP to +40.5‰ at ~12.7 ka BP. During the Younger Dryas event, it climbed again to a maximum measured value of +44.0‰ at ~11.6 ka BP. A sharp decrease then occurred to the lowest value of +39.4‰ at ~10.7 ka BP. $\delta^{18}O_{diatom}$ remained low throughout the early Holocene (~10.7–8.0 ka BP). From ~8.0 to 3.1 ka BP, it increased slowly to a maximum of +42.4‰ at 3.1 ka BP, but then fell again to +40.6‰ at ~1.4 ka BP. The top of the core is missing.

$\delta^{30}Si_{diatom}$ values ranged from +0.62 to +1.26‰ over the last 15 ka BP, giving a total variation of 0.64‰ (Fig. 4). During the late-glacial, $\delta^{30}Si_{diatom}$ was high (+1.04 to +1.24‰), decreasing gradually by 0.30‰ from ~14.9 to 11.6 ka BP. At the start of the Holocene, a further decrease to +0.62‰ at ~10.7 ka BP took place; this represents the lowest $\delta^{30}Si_{diatom}$ value recorded. $\delta^{30}Si_{diatom}$ remained low and relatively stable during the early to mid-Holocene (+0.62 to +0.94‰). From 5.5 ka BP onwards it increased, reaching a maximum of +1.26‰ at ~1.4 ka BP. The relationship between $\delta^{30}Si_{diatom}$ and $\delta^{18}O_{diatom}$, although not directly causal and not statistically significant, shows a trend of increasing $\delta^{30}Si_{diatom}$ with increasing $\delta^{18}O_{diatom}$.

The $P_{wax\ index}$ varied from 0.50 to 0.74, suggesting significant variations in organic-matter sources over the last ~21 ka BP (Fig. 4). During the early part of the record, two intervals of high P_{wax} values (>0.60), dated ~20.1–18.5 and ~16.1–15.7 ka BP, confirm the dominant contribution of leaf waxes from emergent macrophytes/terrestrial plants to the two vertisols present in the core. Elevated P_{aq} (not shown) in the intervening interval, coupled with very low P_{alg} values, suggests very shallow water with abundant submerged/floating macrophytes, which may have shaded out phytoplankton. An abrupt decline to a minimal P_{wax} value (0.52) at ~14.9 ka BP, as the basin reflooded, was followed by a sharp increase to a maximum (0.74) at ~14.1 ka BP. P_{wax} then remained high for several millennia (~14.1–9.7 ka BP) indicating a substantial contribution from terrestrial/emergent plants, before progressively decreasing through the early to mid-Holocene. Although P_{wax} values continued to decline slowly during the late Holocene, they remained fairly stable (0.59–0.63), particularly between ~5.8 and 3 ka BP.

A transient increase in the aquatic, *n*-alkane-based P_{aq} index to 0.65 during the lake transgression (~14.9 ka BP) was followed by an abrupt drop to minimal P_{aq} values (0.36–0.54), which persisted through the late-glacial and early Holocene (~14.1–8.0 ka BP), indicating a dearth of shallow, marginal habitats. From ~7.5 ka BP

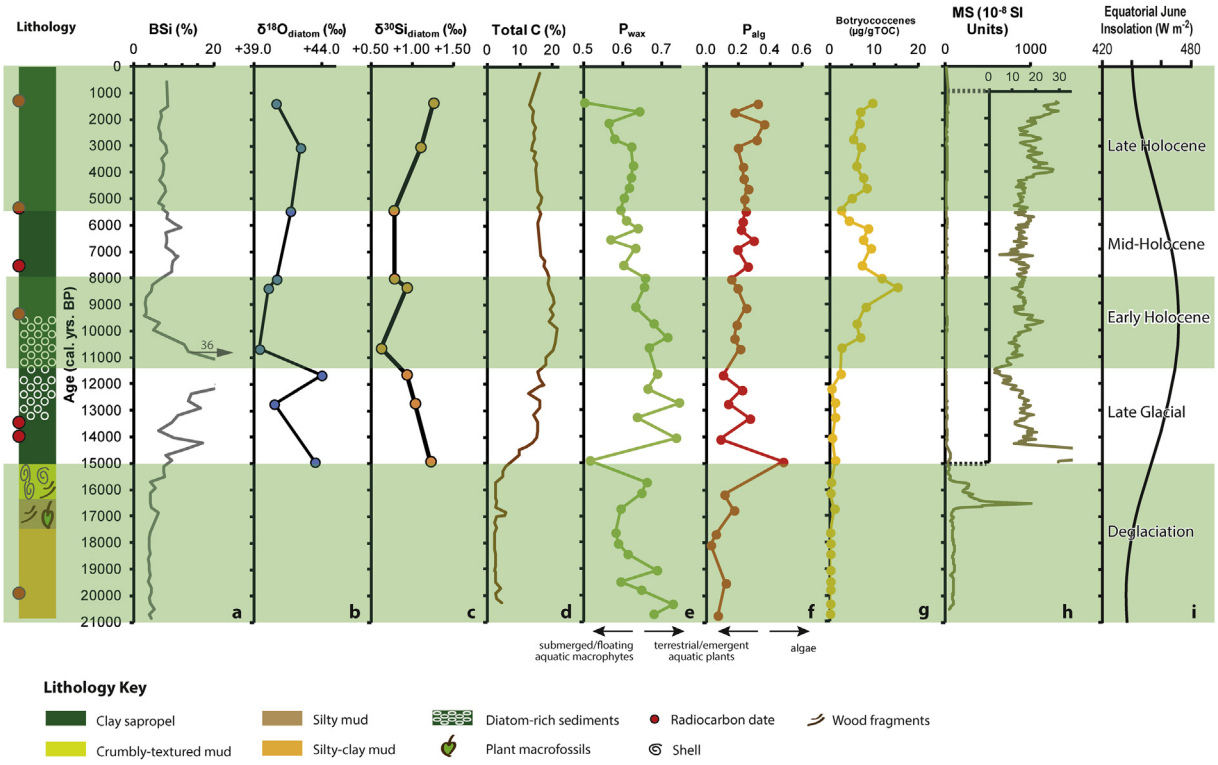

Fig. 4. Variations of sediment composition in Lake Victoria since 21 ka BP compared with orbital forcing: a) BSi content (%) (Johnson et al., 1998); b) $\delta^{18}O_{diatom}$ (‰); c) $\delta^{30}Si_{diatom}$ (‰; d) total C concentration (%) (Johnson et al., 1998); e) P_{wax} index (*n*-alkanes from terrestrial higher plants and emergent macrophytes); f) P_{alg} index (*n*-alkenes from microalgae); g) total concentration of botryococcene compounds (mg/g TOC); h) magnetic susceptibility (10^{-8} SI units) (Ngobi et al., 1998); i) equatorial June insolation (Berger and Loutre, 1991).

onwards, P_{aq} values remained high and fairly stable (0.53–0.69), suggesting an increased prevalence of submerged/floating aquatic plants, especially at the top of the record (~2.2–1.4 ka BP). Algal *n*-alkenes were also found in high abundance in the hydrocarbon fraction. Despite the array of 14 botryococcene compounds (plotted separately in Fig. 4), cyclobotryococcatriene was not identified. A peak in P_{alg} (0.48) at ~14.9 ka BP suggests a transient increase in algal production as the basin floor reflooded. From ~14.1 to 6.6 ka BP, P_{alg} increased gradually from 0.09 to 0.29, remaining fairly stable (0.19–0.26) between 6.1 and 3.1 ka BP. During the last ~3 ka, P_{alg} values were higher ($\leq$0.36) but fluctuating. The two aquatic indicators, P_{alg} and P_{aq}, varied in parallel. An ecological relationship between the algal groups that contributed to P_{alg} and floating/submerged macrophytes is possible given that the latter often support important periphytic algal communities (Brenner et al., 2006; Komárek and Jankovská, 2001).

6.2. Lake Edward

Diatoms form the largest BSi component in Lake Edward sediments (>99%), with the addition of an occasional sponge spicule or phytolith. The diatom assemblages were dominated by a few main genera: *Stephanodiscus*, *Surirella* and *Nitzschia*. *Stephanodiscus* spp. were most abundant in all samples (Fig. 3). A notable shift in species composition between ~5.2 and 4.3 ka BP was observed when purifying diatoms for isotope analysis, from a mixed assemblage with *Stephanodiscus*, *Aulacoseira*, *Surirella*, *Nitzschia*, *Synedra* and *Cymbella* spp. to one dominated by a single taxon, *Stephanodiscus* spp. Of the 21 sample depths selected, 19 proved suitable for O- and Si-isotope analysis. Apart from some frustules that showed signs of breakage during clean-up, notably large *Surirella* spp., the remainder were well preserved with no signs of dissolution or diagenesis (Fig. 3). The most common size fraction used for isotope analysis was 20–38 µm, but the 38–63 and >63 µm fractions were frequently analysed as well, in order to check for diatom species/size effects and contamination by problem components; for example, resistant charcoal particles were encountered in the coarser fractions but absent from the 20–38 µm fraction. In total, including replicates and multiple size fractions, 33 cleaned diatom samples were measured for $\delta^{18}O$ and $\delta^{30}Si$. Based on the replicated samples and the observed relationship of $\delta^{29}Si$ to $\delta^{30}Si$, some samples were removed from the dataset due to erroneous results attributable to contamination by charcoal or silicate minerals. The final Holocene isotope dataset for Lake Edward comprised 26 $\delta^{18}O$ values and 30 $\delta^{30}Si$ values. There were no significant variations in isotope values between size fractions; consequently, the mean value is employed for depths with multiple sub-samples.

During the Holocene, $\delta^{18}O_{diatom}$ varied by 7.2‰ (Fig. 5). Early Holocene (~11.1–7.3 ka BP) values were relatively low and stable, fluctuating only between +36.8 and +38.5‰. Between ~6.9 and 5.6 ka BP, they increased abruptly by 4.6‰, from +35.4 to +40.0‰. A sudden decrease of 3.2‰ between ~5.6 and 5.2 ka BP was followed by an abrupt increase of 3.5‰ to +40.3‰ at 4.4 ka BP. From ~4.4 ka BP onwards, $\delta^{18}O_{diatom}$ increased steadily, attaining its Holocene maximum (+42.6‰) at ~1.9 ka BP and then decreasing very slightly (to +41.6 at ~1.4 ka BP) before reaching +42.2‰ at ~1 ka BP. The uppermost sediments were not retained by the corer.

The Holocene range of $\delta^{30}Si_{diatom}$ values was 1.67‰: from +0.49 to +2.16‰ (Fig. 5). $\delta^{30}Si_{diatom}$ declined from +1.07‰ at ~11.1 ka BP to minimum values of +0.49 to +0.60‰ at ~10.7–9.8 ka BP. Between ~9.8 and 9.5 ka BP, a positive shift of 0.51‰ occurred, leading to a plateau (+0.69 to +1.00‰) that lasted until ~4.4 ka BP. From ~4.4 to 3.4 ka BP, $\delta^{30}Si_{diatom}$ increased by +1.23‰ to its Holocene maximum (+2.16‰), shortly followed by an abrupt decrease to +1.06‰ at ~2.9 ka BP. During the late Holocene (~2.9–1.0 ka BP), it rose again to relatively high values, peaking at +1.99‰ at ~1.4 ka

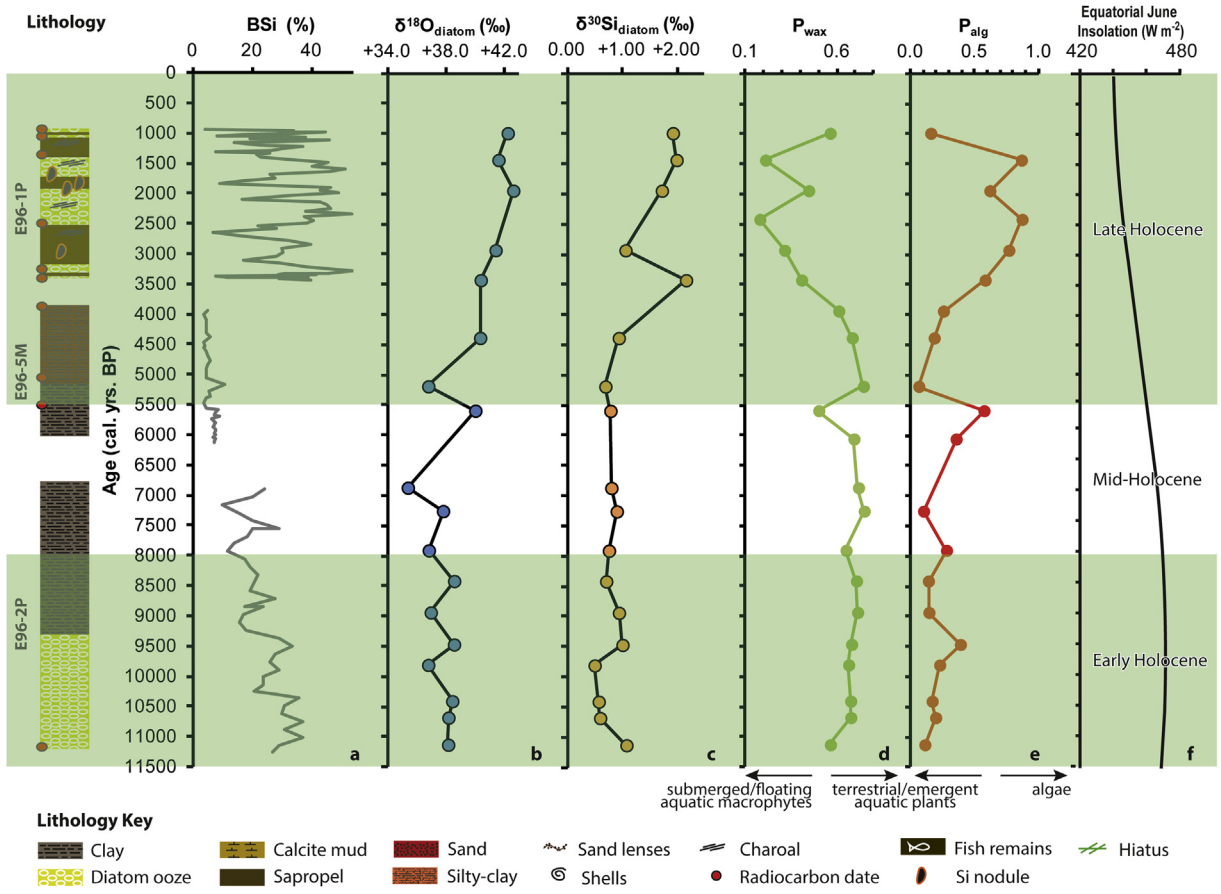

Fig. 5. Variations of sediment composition in Lake Edward since 11.5 ka BP compared with orbital forcing: a) BSi content (%) (Russell et al., 2003a); b) $\delta^{18}O_{diatom}$ (‰); c) $\delta^{30}Si_{diatom}$ (‰); d) P_{wax} index (*n*-alkanes from terrestrial higher plants and emergent macrophytes); e) P_{alg} index (*n*-alkenes from microalgae); f) Equatorial June insolation (Berger and Loutre, 1991).

BP, followed by a small downturn to 1.92‰ by ~1 ka BP. The parallelism between $\delta^{30}Si_{diatom}$ and $\delta^{18}O_{diatom}$ in Lake Edward, while not directly causal, reveals a connection between the processes governing the two isotope systems.

In the Lake Edward sequence, the P_{wax} index varied from 0.18 to 0.75, reflecting major changes in the origin of the organic matter (Fig. 5). At the base of the record (~11.1–10.7 ka BP), P_{wax} values increased from 0.56 to 0.67, remaining high and relatively stable (0.65–0.75) throughout the early to mid-Holocene, implying that leaf waxes from terrestrial or emergent-macrophyte sources predominated. Around 5.6 ka BP, a transient fall to 0.50 suggests a significant aquatic input, after which P_{wax} values reverted to early Holocene levels until ~4.4 ka BP. They then declined to a minimum at ~2.4 ka BP. In the youngest sediments sampled (~2.4–0.9 ka BP), P_{wax} fluctuated greatly but remained relatively low apart from the uppermost sample.

As in Lake Victoria, the two aquatic-biomarker indices P_{aq} (not shown) and P_{alg} varied in parallel, suggesting that they reflect the importance of shallow-water, marginal habitats with abundant aquatic vegetation. At the start of the Holocene (~11.1 ka BP), P_{aq} values were slightly elevated (0.57) but P_{alg} was low (0.11) (Fig. 5). From ~10.7 to 6.1 ka BP, both indicators remained low and stable, marking a prolonged period of reduced input from submerged/floating macrophytes and algae. At ~5.6 ka BP, modest peaks reflect a brief increase in aquatic contributions. Both curves then rose steadily from ~5.2 ka BP to a maximum at ~2.4 ka BP. From ~2.4 ka BP onwards, these aquatic indicators remained high but fluctuating.

7. Interpretation and discussion

The isotope records from diatom silica in Lakes Victoria and Edward are very coherent, although the range of measured values in the two lakes differs in accord with their contrasting geological settings and water-balance types. In the longer (~14.9 ka) but lower-resolution Lake Victoria record, $\delta^{18}O_{diatom}$ varies from +39.4 to +44.0‰, reflecting the very large surface area of the lake and the dominance of evaporative losses in its water budget (Crul, 1995; Nicholson, 1998; Piper et al., 1986; Street-Perrott and Harrison, 1985; Sutcliffe and Parks, 1999). In contrast, the range of $\delta^{18}O_{diatom}$ in the shorter (~11 ka) Lake Edward sequence is wider (from +35.4 to +42.6‰) but the average value is >2‰ lower. Although Lake Edward is situated at a lower altitude, it is fed mainly by high-mountain streams with low $\delta^{18}O$ values (Cockerton et al., 2013), is smaller and deeper, and loses proportionally far more water by surface outflow (Russell and Johnson, 2006; Viner and Smith, 1973). However, as a reservoir-type lake, dependent to a much greater extent on surface inflows than Victoria, it should also have been much more vulnerable to climatic vicissitudes affecting the discharge and $\delta^{18}O$ values of major riverine inputs, such as the inflow from Lake George through the Kazinga Channel (Russell et al., 2003a; Viner, 1977).

The distribution of Si-isotope values in the sediments of the two lakes also differs significantly. $\delta^{30}Si_{diatom}$ values in Lake Victoria (+0.62 to +1.26‰) are on average ~0.4‰ lower than those in Lake Edward (+0.49 to +2.16‰). They also vary over a narrower range (0.64‰), compatible with Rayleigh fractionation in a closed system

such as the epilimnion of a large lake (≤1.1‰) (Alleman et al., 2005; De La Rocha, 2006), whereas the 1.67‰ range of measured values in Lake Edward suggests open-system behaviour (Basile-Doelsch, 2006; Opfergelt et al., 2011; Varela et al., 2004). Superimposed millennial-scale fluctuations of $\delta^{30}Si_{diatom}$ in Lake Edward may record pronounced variations in water and nutrient influxes through the Kazinga Channel. Together, the lower average and range of $\delta^{30}Si_{diatom}$ values observed in Lake Victoria during the late-glacial and Holocene imply a higher ratio of Si supply to demand, as well as a more stable aquatic ecosystem and sedimentation regime, respectively, than in Lake Edward during the Holocene. This contrast may reflect the greater dependence of Lake Edward on highly variable riverine DSi inputs as well as its much shorter DSi residence time (~4 yr as opposed to ~40 yr) (Hecky et al., 1996; Johnson et al., 1998; Russell and Johnson, 2005).

Like the two isotope indicators, the ranges of all three biomarker indices are wider in the Lake Edward sequence than in Lake Victoria, despite the much shorter time span covered (~11 ka *vs.* ~21 ka, respectively). P_{wax} varied from 0.18 to 0.75 (as opposed to 0.50 to 0.74 in Lake Victoria), P_{aq} from 0.36 to 0.93 (*vs.* 0.36 to 0.69) and P_{alg} from 0.10 to 0.87 (*vs.* 0.03 to 0.48). These contrasts confirm the greater sensitivity of Lake Edward to millennial-scale Holocene variations in climate, vegetation and riverine inputs, notably fluctuations in the nutrient-enriched inflow from Lake George (Russell et al., 2003a; Viner, 1977).

Confidence in our isotope and biomarker records is greatly enhanced by their close correspondence with the palaeolimnological records from the two lakes. Past variations in $\delta^{18}O_{diatom}$ agree closely with palaeohydrological indicators such as diatom assemblages (Stager and Johnson, 2008) and δD of leaf waxes (Berke et al., 2012) from Lake Victoria, and mole% Mg and $\delta^{18}O$ in calcite (Russell et al., 2003b) from Lake Edward. Our biomarker data are in good accord with published pollen (Beuning and Russell, 2004; Kendall, 1969) and BSi records (Johnson et al., 1998; Russell et al., 2003a) from both lakes. In turn, our novel Si-isotope analyses support and refine the interpretation of the published BSi concentration data, since the $\delta^{30}Si$ composition of preserved silica is much less affected than BSi concentrations by silica dissolution in the water column and variations in the accumulation rate of other sediment fractions.

During the LGM, consistently low values of P_{alg} in Lake Victoria (Fig. 4) support the stratigraphical evidence (Johnson et al., 1996; Talbot and Lærdal, 2000) for formation of a double vertisol under swampy conditions (high P_{wax}) with an intervening period of very shallow water (high P_{aq}) at the core site. Our sparse $\delta^{18}O_{diatom}$ data confirm the existence of very dry conditions at the start of the lacustrine transgression (~14.9 ka BP) and again during the Younger Dryas stadial (Berke et al., 2012; Johnson et al., 1996; Stager and Johnson, 2008), with an intervening freshening (~12.7 ka BP) during the initial period of lake overflow (Talbot et al., 2000; Williams et al., 2006). ^{14}C- and OSL-dated alluvial deposits in the lower White Nile valley south of Khartoum demonstrate the occurrence of very high Nile flood levels in the interval ~14.5–13 ka BP and to a lesser extent between ~9.7 and 9.1 ka BP (Williams et al., 2015), in good agreement with our $\delta^{18}O_{diatom}$ record from Lake Victoria.

Despite increasing concentrations of BSi in core V95-1P (Johnson et al., 1998), $\delta^{30}Si_{diatom}$ declined by 0.6‰ between ~14.9 and 10.7 ka BP (Fig. 4), an unexpected result indicating that DSi supply increased to levels that greatly exceeded aquatic demand and/or that the $\delta^{30}Si$ values of riverine DSi inputs fell significantly. Several explanations can be advanced for this isotopic change. First, deep-rooted vascular plants, especially tropical forests, greatly enhance rates of chemical weathering and ecosystem Si cycling (Alexandre et al., 1997; Kelly et al., 1998; Lucas, 2001). During the late-glacial, as JJA insolation, air temperature and monsoon rainfall increased (Berke et al., 2012), montane rainforest and ericaceous shrubland expanded at high altitudes (Jolly et al., 1997), while semi-deciduous forest replaced savanna grassland around Lake Victoria (Kendall, 1969), driving up P_{wax} (Fig. 4). Recent work in Belgium suggests that development of climax forest both increases DSi fluxes to streams (Struyf et al., 2010) and decreases the $\delta^{30}Si$ values of soil water, due to intense recycling of isotopically depleted BSi and secondary silicates (Vandevenne et al., 2015). We hypothesize that a warmer, more humid climate with increased woody vegetation cover boosted dissolution of phytoliths and silicate minerals in weathering-limited, high-altitude regions, as well as enhancing the flushing of isotopically depleted DSi from transport-limited, deep soil mantles in the equatorial lowlands (cf. Street-Perrott and Barker, 2008). Secondly, refilling of the lake basin after ~15 ka BP (Berke et al., 2012; Johnson et al., 1996; Stager and Johnson, 2008) may have remobilized large amounts of isotopically depleted BSi from newly flooded wetland soils (Frings et al., 2014b; Struyf et al., 2015). Thirdly, Lake Victoria overflowed into the White Nile from ~14.2 to 14 ka BP onwards (Talbot et al., 2000; Williams et al., 2006), shortening the residence time of DSi in the waterbody (Beuning and Russell, 2004).

At first sight, it is puzzling that the cold/dry Younger Dryas event (~13–11.5 ka BP), which is clearly represented in Lake Victoria by its fossil diatom assemblages (Stager et al., 1997) and the $\delta^{18}O$ peak at ~11.6 ka BP, barely registered in the Si-isotope curve from core V95-1P, even though sedimentary BSi concentrations reached their highest levels (Fig. 4). The persistence of low $\delta^{30}Si_{diatom}$ values suggests that the riverine DSi flux continued to exceed diatom demand during this interval. A lack of clastic sedimentation to dilute the accumulating BSi is implied by a minimum in magnetic susceptibility (MS) in this core (Fig. 4). However, the rather weak Younger Dryas signal in the pollen record from Lake Victoria (Kendall, 1969) implies that terrestrial vegetation, chemical weathering, Si cycling and erosion in its vast catchment exhibited a slower and more muted response than lake level to this abrupt fluctuation in climate.

The early to mid-Holocene (~11.5–5.5 ka BP) was the warmest and wettest period of the last 20 ka in the upper White Nile drainage (Berke et al., 2012). High groundwater levels and local wetlands persisted until ~6 ka BP in areas adjacent to the lower White Nile valley (Williams et al., 2015). Both our lake records display persistently low and parallel $\delta^{18}O_{diatom}$ and $\delta^{30}Si_{diatom}$ curves, alongside high values of P_{wax} (Figs. 4 and 5). In the Lake Victoria basin, the P_{wax} curve reflects the dominance of humid, evergreen rainforest, whereas Lake Edward was surrounded by moist semi-deciduous forest, suggesting high chemical-weathering rates and riverine DSi fluxes in both catchments. Both lakes were extensive and overflowing.

Paradoxically, however, BSi concentrations fell to their lowest measured levels in core V95-1P during the early Holocene. A peak of botryococcenes dated ~10.3–6.1 ka BP (Fig. 4) confirms palaeoecological data showing that *B. braunii* and other green algae outcompeted diatoms in Lake Victoria (Johnson et al., 1998, 2000). Johnson et al. (2000) suggested that increased stratification of the water column due to low wind strength or intense surface heating might have prevented diatoms from remaining in suspension or negated their competitive advantage at withstanding mixing: a hypothesis applicable to both lakes. However, replacement of *Stephanodiscus astraea* as the dominant diatom taxon by more Si-demanding *Aulacoseira* spp. (Kilham et al., 1986) reinforces the evidence from minimal $\delta^{30}Si$ values that Si concentrations were not limiting ($\delta^{30}Si_{diatom}$ rises when aquatic demand for DSi exceeds supply); hence, nutrient stoichiometry may have shifted in favour of other algal groups. In Lake Malawi, for example, cyanobacteria and green algae outcompete diatoms during the

modern rainy season, when the lake is strongly stratified and nutrient levels are low (Stone et al., 2011). Here, we propose that the dominance of stable forest, lake and swamp environments in the upper White Nile catchments during the early to mid-Holocene (Beuning and Russell, 2004; Beuning et al., 1997; Jolly et al., 1997; Kendall, 1969), while it enhanced chemical weathering and hence DSi supply, simultaneously minimized riverine influxes of soil-derived particulate and soluble P (cf. Haberyan and Hecky, 1987), thereby promoting dominance of Lake Victoria by green algae, which only need moderate amounts of P and do not deplete DSi. The colonial alga *B. braunii* is particularly buoyant and can thrive in very oligotrophic waters with low P, C and N concentrations (Smittenberg et al., 2005; Street-Perrott et al., 2007 and references therein).

After the end of the AHP (~5.5 ka), insolation forcing, monsoon intensity, forest cover and P_{wax} all declined, while $\delta^{18}O_{diatom}$ increased in Lakes Victoria and Edward, testifying to a decrease in P/E (Figs. 4 and 5). Parallel increases in P_{aq} and P_{alg} in both sequences reflect the expansion of marginal shallows in which submerged/floating macrophyte communities supported periphytic algae (Stager, 1984; Stager and Johnson, 2000). Higher $\delta^{30}Si_{diatom}$ values suggest a decrease in the $\delta^{30}Si$ values of riverine inputs and/or a fall in DSi supply relative to aquatic demand, reversing the trends seen in the late-glacial to early Holocene. Downstream, the long sequence of Mesolithic and Neolithic occupation of the White Nile Valley and adjacent wetlands had essentially ended by ~6 ka BP (Williams et al., 2015). During the late Holocene, the millennial-scale fluctuations of $\delta^{30}Si_{diatom}$ observed in Lake Edward may have been magnified by variations in water and nutrient influx through the Kazinga Channel. In particular, its Si-isotope maximum at ~3.4 ka BP may reflect complete desiccation of Lake George (Viner, 1977), cutting off fluvial DSi inputs derived from its Rwenzori tributaries and the activity of grazing hippos.

These natural changes in terrestrial vegetation and Si cycling were reinforced by deforestation by pioneer Iron-Age farmers beginning ~3 ka BP (Jolly et al., 1997; Taylor et al., 2000), or possibly even earlier (Lejju et al., 2006). After an initial transient response, forest degradation and conversion to cropland can be expected to decrease long-term DSi export fluxes (Struyf et al., 2010), while increasing riverine $\delta^{30}Si$ values (Vandevenne et al., 2015) and P fluxes (Brenner et al., 2006; Sharpley et al., 1995; Smil, 2000), thereby leading to lake eutrophication (elevated P_{aq}, P_{alg}) and raised $\delta^{30}Si_{diatom}$ values.

Overall, a comparison of our novel $\delta^{30}Si_{diatom}$ records with the corresponding variations in JJA insolation, $\delta^{18}O_{diatom}$ and P_{wax} (Figs. 4 and 5) provides evidence that the major stages in the late-glacial and Holocene evolution of the Si cycle in the upper White Nile basin were driven by orbital forcing of climate and associated land-surface feedbacks acting on a multi-millennial time scale, together with superimposed sub-Milankovitch fluctuations in temperature and monsoon rainfall of sufficient magnitude and duration to impact significantly on terrestrial ecosystems and be registered at ~500 yr sampling resolution. The late Holocene arrival of agriculture and iron smelting may merely have enhanced the impact of declining monsoon rainfall. A very similar $\delta^{30}Si_{diatom}$ curve was obtained by Swann et al. (2010) from Lake El'gygytgyn, Siberia, hinting that significant Late Quaternary variations in the continental Si cycle were driven by global climate change through its influence on rates of chemical weathering and nutrient mobilization. However, many more Si-isotope records will be needed in order to confirm this hypothesis.

8. Conclusions

The isotopic changes recorded in the sediments of these large lakes, located at the head of one of the world's principal river systems, demonstrate the interaction of global climate with a major biogeochemical cycle at multi-millennial to millennial time scales. If other large river systems were similarly affected, the regulation of the silicon cycle by terrestrial and freshwater ecosystems may have been a major determinant not only of DSi export from the continents to the oceans, but also of its mean Si-isotope value. Given the significant role played by diatoms in drawing down CO_2 in the oceans, where they account for ~20% of net primary productivity, natural perturbations of the continental silicon cycle may have had direct feedback effects on the carbon cycle, and hence on global changes initiated by orbital forcing and major atmosphere–ocean reorganizations.

Acknowledgements

This work was supported by the UK Natural Environment Research Council through a Doctoral Training Grant (HEC) and a grant-in-kind from the NERC Isotope Geosciences Facilities Steering Committee (IP-1151-1109) for O-, H- and Si-isotope analyses (FAS-P). A Research and Exploration Grant from the National Geographic Society (FAS-P) funded fieldwork in the Nile Basin. We thank the LacCore staff for assisting efficiently with sample selection and despatch, and Tom Johnson and Jim Russell for sharing their expertise and data relating to the Lake Victoria and Edward cores. Andrea Snelling provided helpful advice on diatom extraction from difficult samples. We also thank two anonymous referees for their positive comments, which have improved the paper.

References

Alexandre, A., Meunier, J.-D., Colin, F., Koud, J.-M., 1997. Plant impact on the biogeochemical cycle of silicon and related weathering processes. Geochim. Cosmochim. Acta 61, 677–682.
Alleman, L.Y., Cardinal, D., Cocquyt, C., Plisnier, P.-D., Descy, J.-P., Kimirei, I., Sinyinza, D., André, L., 2005. Silicon isotopic fractionation in Lake Tanganyika and its main tributaries. J. Gt. Lakes Res. 31, 509–519.
Bard, E., Rostek, F., Turon, J.-L., Gendreau, S., 2000. Hydrological impact of Heinrich events in the subtropical northeast Atlantic. Science 289, 1321–1324.
Barker, P.A., Hurrell, E.R., Leng, M.J., Wolff, C., Cocquyt, C., Sloane, H.J., Verschuren, D., 2011. Seasonality in equatorial climate over the past 25 k.y. revealed by oxygen isotope records from Mount Kilimanjaro. Geology 39, 1111–1114.
Barker, P.A., Leng, M.J., Gasse, F., Huang, Y., 2007. Century-to-millennial scale climatic variability in Lake Malawi revealed by isotope records. Earth Planet. Sci. Lett. 261, 93–103.
Barker, P.A., Street-Perrott, F.A., Leng, M.J., Greenwood, P.B., Swain, D.L., Perrott, R.A., Telford, R.J., Ficken, K.J., 2001. A 14,000-year oxygen isotope record from diatom silica in two alpine lakes on Mt. Kenya. Science 292, 2307–2310.
Barker, P.A., Talbot, M.R., Street-Perrott, F.A., Marret, F., Scourse, J., Odada, E.O., 2004. Late Quaternary climatic variability in intertropical Africa. In: Battarbee, R.W., Gasse, F., Stickley, C.E. (Eds.), Past Climate Variability Through Europe and Africa. Springer, Dordrecht, pp. 117–138.
Basile-Doelsch, I., 2006. Si stable isotopes in the Earth's surface: a review. J. Geochem. Explor. 88, 252–256.
Berger, A., Loutre, M.F., 1991. Insolation values for the last 10 million years. Quat. Sci. Rev. 10, 297–317.
Berke, M.A., Johnson, T.C., Werne, J.P., Grice, K., Schouten, S., Sinninghe Damsté, J.S., 2012. Molecular records of climate variability and vegetation response since the Late Pleistocene in the Lake Victoria Basin, East Africa. Quat. Sci. Rev. 55, 59–74.
Berner, E.K., Berner, R.A., 2012. Global Environment: Water, Air, and Geochemical Cycles, second ed. Princeton University Press, Princeton.
Beuning, K.R.M., Kelts, K., Russell, J., Wolfe, B.B., 2002. Reassessment of Lake Victoria-Upper Nile River paleohydrology from oxygen isotope records of lake-sediment cellulose. Geology 30, 559–562.
Beuning, K.R.M., Russell, J.M., 2004. Vegetation and sedimentation in the Lake Edward Basin, Uganda-Congo during the late Pleistocene and early Holocene. J. Paleolimnol. 32, 1–18.
Beuning, K.R.M., Talbot, M.R., Kelts, K., 1997. A revised 30,000-year paleoclimatic and paleohydrologic history of Lake Albert, East Africa. Palaeogeogr. Palaeoclimatol. Palaeoecol. 136, 259–279.
Bond, G., Heinrich, H., Broecker, W., Labeyrie, L., McManus, J., Andrews, J., Huon, S., Jantschik, R., Clasen, S., Simet, C., Tedesco, K., Kias, M., Bonani, G., Ivy, S., 1992. Evidence for massive discharges of icebergs into the North Atlantic ocean during the last glacial period. Nature 360, 245–249.

Bootsma, H.A., 2003. Inputs, outputs, and internal cycling of silica in a large, tropical lake. J. Gt. Lakes Res. 29, 121–138.
Brandriss, M.E., O'Neil, J.R., Edlund, M.B., Stoermer, E.F., 1998. Oxygen isotope fractionation between diatomaceous silica and water. Geochim. Cosmochim. Acta 62, 1119–1125.
Brenner, M., Hodell, D.A., Leyden, B.W., Curtis, J.H., Kenney, W.F., Gu, B., Newman, J.M., 2006. Mechanisms for organic matter and phosphorus burial in sediments of a shallow, subtropical, macrophyte-dominated lake. J. Paleolimnol. 35, 129–148.
Brzezinski, M.A., Pride, C.J., Franck, V.M., Sigman, D.M., Sarmiento, J.L., Matsumoto, K., Gruber, N., Rau, G.H., Coale, H.K., 2002. A switch from Si(OH)4 to NO3- depletion in the glacial Southern Ocean. Geophys. Res. Lett. 29, 1564.
Carey, J.C., Fulweiler, R.W., 2012. The terrestrial silica pump. PLoS One. Public Library of Science e52932.
Chapligin, B., Leng, M.J., Webb, E., Alexandre, A., Dodd, J.P., Ijiri, A., Lücke, A., Shemesh, A., Abelmann, A., Herzschuh, U., Longstaffe, F.J., Meyer, H., Moschen, R., Okazaki, Y., Rees, N.H., Sharp, Z.D., Sloane, H.J., Sonzogni, C., Swann, G.E.A., Sylvestre, F., Tyler, J.J., Yam, R., 2011. Inter-laboratory comparison of oxygen isotope compositions from biogenic silica. Geochim. Cosmochim. Acta 75, 7242–7256.
Chen, J., Li, J., Tian, S., Kalugin, I., Darin, A., Xu, S., 2012. Silicon isotope composition of diatoms as a paleoenvironmental proxy in Lake Huguangyan, South China. J. Asian Earth Sci. 45, 268–274.
Clayton, R.N., Mayeda, T.K., 1963. The use of bromine pentafluoride in the extraction of oxygen from oxides and silicates from isotopic analysis. Geochim. Cosmochim. Acta 27, 43–52.
Cockerton, H.E., Street-Perrott, F.A., Leng, M.J., Barker, P.A., Horstwood, M.S.A., Pashley, V., 2013. Stable-isotope (H, O, and Si) evidence for seasonal variations in hydrology and Si cycling from modern waters in the Nile Basin: implications for interpreting the Quaternary record. Quat. Sci. Rev. 66, 4–21.
Conley, D.J., 1997. Riverine contribution of biogenic silica to the oceanic silica budget. Limnol. Oceanogr. 42, 774–777.
Conley, D.J., 2002. Terrestrial ecosystems and the global biogeochemical silica cycle. Glob. Biogeochem. Cycles 16, 68-61–68-69.
Cornelis, J.-T., Delvaux, B., Georg, R.B., Lucas, Y., Ranger, J., Opfergelt, S., 2011. Tracing the origin of dissolved silicon transferred from various soil-plant systems towards rivers: a review. Biogeosciences 8, 89–112.
Cranwell, P.A., Eglinton, G., Robinson, N., 1987. Lipids of aquatic organisms as potential contributors to lacustrine sediments. Org. Geochem. 11, 513–527.
Crul, R.C.M., 1995. Management and Conservation of the African Great Lakes: Lakes Victoria, Tanganyika and Malawi. IHP-IV project M-5-1. UNESCO, p. 107.
De La Rocha, C., Tréguer, P.J., 2012. The world ocean silica cycle. Annu. Rev. Mar. Sci. 5, 477–501.
De La Rocha, C.L., 2002. Tracing the silica cycle with silicon isotopes. Océanis 28, 369–389.
De La Rocha, C.L., 2006. Opal-based isotopic proxies of paleoenvironmental conditions. Glob. Biogeochem. Cycles 20, GB4S09.
De La Rocha, C.L., Bickle, M.J., 2005. Sensitivity of silicon isotopes to whole-ocean changes in the silica cycle. Mar. Geol. 217, 267–282.
De La Rocha, C.L., Brzezinski, M.A., DeNiro, M.J., 2000. A first look at the distribution of the stable isotopes of silicon in natural waters. Geochim. Cosmochim. Acta 64, 2467–2477.
De La Rocha, C.L., Brzezinski, M.A., DeNiro, M.J., Shemesh, A., 1998. Silicon-isotope composition of diatoms as an indicator of past oceanic change. Nature 395, 680–683.
de Mesmay, R., Grossi, V., Williamson, D., Kajula, S., Derenne, S., 2007. Novel mono-, di- and tri-unsaturated very long chain (C_{37}–C_{43}) *n*-alkenes in alkenone-free lacustrine sediments (Lake Masoko, Tanzania). Org. Geochem. 38, 323–333.
deMenocal, P., Ortiz, J., Guilderson, T., Adkins, J., Sarnthein, M., Baker, L., Yarusinsky, M., 2000. Abrupt onset and termination of the African Humid Period: rapid climate responses to gradual insolation forcing. Quat. Sci. Rev. 19, 347–361.
Derry, L.A., Kurtz, A.C., Ziegler, K., Chadwick, O.A., 2005. Biological control of terrestrial silica cycling and export fluxes to watersheds. Nature 433, 728–731.
Dessert, C., Dupré, B., Gaillardet, J., François, L., Allègre, C.J., 2003. Basalt weathering laws and the impact of basalt weathering on the global carbon cycle. Chem. Geol. 202, 257–273.
Ding, T.P., Jiang, S.Y., Wan, D.F., Li, Y.H., Li, J.C., Song, H.B., Liu, Z.J., Yao, X.M., 1996. Silicon Isotope Geochemistry. Geological Publishing House, Beijing.
Ding, T.P., Wan, D.F., Wang, C., Zhang, F., 2004. Silicon isotope compositions of dissolved silicon and suspended matter in the Yangtse River, China. Geochim. Cosmochim. Acta 68, 205–216.
Douthitt, C.B., 1982. The geochemistry of the stable isotopes of silicon. Geochim. Cosmochim. Acta 46, 1449–1458.
Dupré, B., Dessert, C., Oliva, P., Goddéris, Y., Viers, J., François, L.M., Millot, R., Gaillardet, J., 2003. Rivers, chemical weathering and Earth's climate. C. R. Geosci. 335, 1141–1160.
Eglinton, G., Hamilton, R.J., 1967. Leaf epicuticular waxes. Science 156, 1322–1335.
Ficken, K.J., Li, B., Swain, D.L., Eglinton, G., 2000. An *n*-alkane proxy for the sedimentary input of submerged/floating freshwater aquatic macrophytes. Org. Geochem. 31, 745–749.
Ficken, K.J., Street-Perrott, F.A., Perrott, R.A., Swain, D.L., Olago, D.O., Eglinton, G., 1998. Glacial/interglacial variations in carbon cycling revealed by molecular and isotope stratigraphy of Lake Nkunga, Mt. Kenya, East Africa. Org. Geochem. 29, 1701–1719.
Flohn, H., Fraedrich, K., 1966. Tagesperiodische Zirkulation und Niederschlagsverteilung am Viktoria-See (Ostafrika). Meteorol. Rundsch. 19, 157–165.
Fontorbe, G., De La Rocha, C.L., Chapman, H.J., Bickle, M.J., 2013. The silicon isotopic composition of the Ganges and its tributaries. Earth Planet. Sci. Lett. 381, 21–30.
Frings, P.J., Clymans, W., Jeppesen, E., Lauridsen, T.L., Struyf, E., Conley, D.J., 2014a. Lack of steady-state in the global biogeochemical Si cycle: emerging evidence from lake Si sequestration. Biogeochemistry 117, 255–277.
Frings, P.J., De La Rocha, C., Struyf, E., van Pelt, D., Schoelynck, J., Hudson, M.M., Gondwe, M.J., Wolski, P., Mosimane, K., Gray, W., Schaller, J., Conley, D.J., 2014b. Tracing silicon cycling in the Okavango Delta, a sub-tropical flood-pulse wetland using silicon isotopes. Geochim. Cosmochim. Acta 142, 132–148.
Froelich, P.N., Blanc, V., Mortlock, R.A., Chillrud, S.N., Dunstan, W., Udomkit, A., Peng, T.-H., 1992. River fluxes of dissolved silicate to the ocean were higher during glacials: Ge/Si in diatoms, rivers and oceans. Paleoceanography 7, 739–767.
Gaillardet, J., Dupré, B., Louvat, P., Allègre, C.J., 1999. Global silicate weathering and CO_2 consumption rates deduced from the chemistry of large rivers. Chem. Geol. 159, 3–30.
Garzanti, E., Padoan, M., Andò, S., Resentini, A., Vezzoli, G., Lustrino, M., 2013a. Weathering and relative durability of detrital minerals in equatorial climate: sand petrology and geochemistry in the East African Rift. J. Geol. 121, 547–580.
Garzanti, E., Padoan, M., Peruta, L., Setti, M., Najman, Y., Villa, I.M., 2013b. Weathering geochemistry and Sr-Nd fingerprints of equatorial upper Nile and Congo muds. Geochem. Geophys. Geosyst. 14, 292–316.
Gasse, F., 2000. Hydrological changes in the African tropics since the Last Glacial Maximum. Quat. Sci. Rev. 19, 189–211.
Gasse, F., Chalié, F., Vincens, A., Williams, M.A.J., Williamson, D., 2008. Climatic patterns in equatorial and southern Africa from 30,000 to 10,000 years ago reconstructed from terrestrial and near-shore proxy data. Quat. Sci. Rev. 27, 2316–2340.
Green, J., 2009. Nilotic lakes of the Western Rift. In: Dumont, H.J. (Ed.), The Nile: Origin, Environments, Limnology and Human Use. Springer Science + Business Media B.V, pp. 263–286.
Haberyan, K.A., Hecky, R.E., 1987. The Late Pleistocene and Holocene stratigraphy and paleolimnology of Lakes Kivu and Tanganyika. Palaeogeogr. Palaeoclimatol. Palaeoecol. 61, 169–197.
Hecky, R.E., Bootsma, H.A., Mugidde, R.M., Bugenyi, F.W.B., 1996. Phosphorus pumps, nitrogen sinks and silicon drains: plumbing nutrients in the African Great Lakes. In: Johnson, T.C., Odada, E.O., Whittaker, K.T. (Eds.), The Limnology, Climatology and Paleoclimatology of the East African Lakes. Gordon and Breach, Amsterdam, pp. 205–224.
Hecky, R.E., Degens, E.T., 1973. Late Pleistocene-Holocene Chemical Stratigraphy and Paleolimnology of the Rift Valley Lakes of Central Africa. Woods Hole Oceanographic Institution Technical Report WHOI-73-28, Woods Hole, Massachusetts, p. 138.
Hernández, A., Bao, R., Giralt, S., Barker, P.A., Leng, M.J., Sloane, H.J., Sáez, A., 2011. Biogeochemical processes controlling oxygen and carbon isotopes of diatom silica in Late Glacial to Holocene lacustrine rhythmites. Palaeogeogr. Palaeoclimatol. Palaeoecol. 299, 413–425.
Hernández, A., Giralt, S., Bao, R., Sáez, A., Leng, M.J., Barker, P.A., 2010. ENSO and solar activity signals from oxygen isotopes in diatom silica during late glacial-Holocene transition in Central Andes (18°S). J. Paleolimnol. 44, 413–429.
Huang, Y., Street-Perrott, F.A., Perrott, R.A., Metzger, P., Eglington, G., 1999. Glacial–interglacial environmental changes inferred from molecular and compound-specific $\delta^{13}C$ analyses of sediments from Sacred Lake, Mt. Kenya. Geochim. Cosmochim. Acta 63, 1383–1404.
Hughes, H.J., Bouillon, S., André, L., Cardinal, D., 2012. The effects of weathering variability and anthropogenic pressures upon silicon cycling in an intertropical watershed (Tana River, Kenya). Chem. Geol. 308–309, 18–25.
Hughes, H.J., Sondag, F., Cocquyt, C., Laraque, A., Pandi, A., André, L., Cardinal, D., 2011. Effect of seasonal biogenic silica variations on dissolved silicon fluxes and isotopic signatures in the Congo River. Limnol. Oceanogr. 56, 551–561.
Hughes, H.J., Sondag, F., Santos, R.V., André, L., Cardinal, D., 2013. The riverine silicon isotope composition of the Amazon Basin. Geochim. Cosmochim. Acta 121, 637–651.
Hughes, R.H., Hughes, J.S., 1992. A Directory of African Wetlands. IUCN, Gland, Switzerland and Cambridge, UK/UNEP, Nairobi, Kenya/WCMC, Cambridge, UK.
Humborg, C., Conley, D., Rahm, L., Wulff, F., Cociasu, A., Ittekkot, V., 2000. Silicon retention in river basins: far-reaching effects on biogeochemistry and aquatic food webs in coastal marine environments. Ambio 29, 45–50.
Johnson, T.C., 1996. Sedimentary processes and signals of past climatic changes in the large lakes of the East African Rift Valley. In: Johnson, T.C., Odada, E.O. (Eds.), The Limnology, Climatology and Paleoclimatology of the East African Lakes. Gordon and Breach Publishers, Amsterdam, The Netherlands, pp. 367–412.
Johnson, T.C., Barry, S.L., Chan, Y., Wilkinson, P., 2001. Decadal record of climate variability spanning the past 700 yr in the Southern Tropics of East Africa. Geology 29, 83–86.
Johnson, T.C., Brown, E.T., McManus, J., Barry, S., Barker, P., Gasse, F., 2002. A high-resolution paleoclimate record spanning the past 25,000 years in southern East Africa. Science 296, 113–132.
Johnson, T.C., Chan, Y., Beuning, K., Kelts, K., Ngobi, G., Verschuren, D., 1998. Biogenic silica profiles in Holocene cores from Lake Victoria: implications for lake level history and initiation of the Victoria Nile. In: Lehman, J.T. (Ed.), Environmental Change and Response in East African Lakes. Kluwer Press, Amsterdam, pp. 75–88.

Johnson, T.C., Kelts, K., Odada, E., 2000. The Holocene history of Lake Victoria. Ambio 29, 2–11.
Johnson, T.C., Scholz, C.A., Talbot, M., Kelts, K., Ricketts, R.D., Ngobi, G., Beuning, K., Ssemmanda, I., McGill, J.W., 1996. Late Pleistocene desiccation of Lake Victoria and rapid evolution of cichlid fishes. Science 273, 1091–1093.
Jolly, D., Taylor, D., Marchant, R., Hamilton, A., Bonnefille, R., Buchet, G., Riollet, G., 1997. Vegetation dynamics in central Africa since 18,000 yr BP: pollen records from the interlacustrine highlands of Burundi, Rwanda and western Uganda. J. Biogeogr. 24, 492–512.
Kelly, E.F., Chadwick, O.A., Hilinski, T.E., 1998. The effect of plants on mineral weathering. Biogeochemistry 42, 21–53.
Kelts, K., Hsü, K.J., 1978. Freshwater carbonate sedimentation. In: Lerman, A. (Ed.), Lakes: Chemistry, Geology, Physics. Springer-Verlag, New York, pp. 295–323.
Kendall, R.L., 1969. An ecological history of the Lake Victoria basin. Ecol. Monogr. 39, 121–176.
Kiage, L.M., Liu, K.-B., 2006. Late Quaternary paleoenvironmental changes in East Africa: a review of multiproxy evidence from palynology, lake sediments, and associated records. Prog. Phys. Geogr. 30, 633–658.
Kilham, P., Kilham, S.S., Hecky, R.E., 1986. Hypothesized resource relationships among African planktonic diatoms. Limnol. Oceanogr. 31, 1169–1181.
Komárek, J., Jankovská, V., 2001. Review of the green algal genus *Pediastrum*: implication for pollen-analytical research. Bibl. Phycol. 108, 1–127.
Kump, L.R., Kasting, J.F., Crane, R.G., 2013. The Earth System, third ed. Pearson, Harlow.
Kutzbach, J.E., Street-Perrott, F.A., 1985. Milankovitch forcing of fluctuations in the level of tropical lakes from 18 to 0 kyr BP. Nature 317, 130–134.
Lærdal, T., Talbot, M.R., 2002. Basin neotectonics of Lakes Edward and George. East Afr. Rift 187, 213–232.
Lærdal, T., Talbot, M.R., Russell, J.M., 2002. Late Quaternary sedimentation and climate in the Lakes Edward and George area, Uganda-Congo. In: Odada, E.O., Olago, D.O. (Eds.), The East African Great Lakes: Limnology, Palaeolimnology and Biodiversity. Springer, Netherlands, pp. 429–470.
Langdale-Brown, I., Osmaston, H.A., W, J.G., 1964. The Vegetation of Uganda and Its Bearing on Land Use. Government of Uganda, Entebbe.
Laruelle, G.G., Roubeix, V., Sferratore, A., Brodherr, B., Ciuffa, D., Conley, D.J., Dürr, H.H., Garnier, J., Lancelot, C., Le Thi Phuong, Q., Meunier, J.D., Meybeck, M., Michalopoulos, P., Moriceau, B., Ní Longphuirt, S., Loucaides, S., Papush, L., Presti, M., Ragueneau, O., Regnier, P., Saccone, L., Slomp, C.P., Spiteri, C., Van Cappellen, P., 2009. Anthropogenic perturbations of the silicon cycle at the global scale: key role of the land-ocean transition. Glob. Biogeochem. Cycles 23, GB4031.
Lehman, J.T., 2002. Application of satellite AVHRR to water balance, mixing dynamics, and the chemistry of Lake Edward, East Africa. In: Odada, E.O., Olago, D. (Eds.), The East African Great Lakes: Limnology, Palaeolimnology and Biodiversity. Kluwer Academic Publishers, The Netherlands, pp. 235–260.
Lejju, B.J., Robertshaw, P., Taylor, D., 2006. Africa's earliest bananas? J. Archaeol. Sci. 33, 102–113.
Leng, M.J., Barker, P.A., 2006. A review of the oxygen isotope composition of lacustrine diatom silica for palaeoclimate reconstruction. Earth Sci. Rev. 75, 5–27.
Leng, M.J., Marshall, J.D., 2004. Palaeoclimate interpretation of stable isotope data from lake sediment archives. Quat. Sci. Rev. 23, 811–831.
Leng, M.J., Sloane, H.J., 2008. Combined oxygen and silicon isotope analysis of biogenic silica. J. Quat. Sci. 23, 313–319.
Leng, M.J., Swann, G.E.A., Hodson, M.J., Tyler, J.J., Patwardhan, S.V., Sloane, H.J., 2009. The potential use of silicon isotope composition of biogenic silica as a proxy for environmental change. Silicon 1, 65–77.
Livingstone, D., 1967. Postglacial vegetation of the Ruwenzori Mountains in equatorial Africa. Ecol. Monogr. 37, 25–52.
Lucas, Y., 2001. The role of plants in controlling rates and products of weathering: importance of biological pumping. Annu. Rev. Earth Planet. Sci. 29, 135–163.
Lupker, M., France-Lanord, C., Galy, V., Lavé, J., Kudrass, H., 2013. Increasing chemical weathering in the Himalayan system since the Last Glacial Maximum. Earth Planet. Sci. Lett. 365, 243–252.
Matsumoto, G.I., Akiyama, M., Watanuki, K., Torii, T., 1990. Unusual distributions of long-chain *n*-alkanes and *n*-alkenes in Antarctic soil. Org. Geochem. 15, 403–412.
Meyers, P.A., 1997. Organic geochemical proxies of paleoceanographic, paleolimnologic and paleoclimatic processes. Org. Geochem. 27, 213–250.
Meyers, P.A., Ishiwatari, R., 1993. Lacustrine organic geochemistry: an overview of indicators of organic matter sources and diagenesis in lake sediments. Org. Geochem. 20, 867–900.
Morley, D.W., Leng, M.J., Mackay, A.W., Sloane, H.J., Rioual, P., Battarbee, R.W., 2004. Cleaning lake sediment samples for diatom oxygen isotope analysis. J. Paleolimnol. 31, 391–401.
Moschen, R., Lücke, A., Schleser, G.H., 2005. Sensitivity of biogenic silica oxygen isotopes to changes in surface water temperature and paleoclimatology. Geophys. Res. Lett. 32.
Ngobi, G.N., Kelts, K., Johnson, T.C., Solheid, P.A., 1998. Environmental magnetism of Late Pleistocene/Holocene sequences from Lake Victoria, East Africa. In: Lerman, J.T. (Ed.), Environmental Change and Response in East African Lakes. Kluwer, Amsterdam.
Nicholson, S.E., 1996. A review of climate dynamics and climate variability in Eastern Africa. In: Johnson, T.C., Odada, E.O. (Eds.), The Limnology, Climatology and Paleoclimatology of the East African Lakes. Gordon and Breach Publishers, Amsterdam, The Netherlands, pp. 25–56.
Nicholson, S.E., 1998. Historical fluctuations of Lake Victoria and other lakes in the northern rift valley of East Africa. In: Lehman, J.T. (Ed.), Environmental Change and Response in East African Lakes. Kluwer Academic Publishers, The Netherlands, pp. 7–35.
Opfergelt, S., Eiriksdottir, E.S., Burton, K.W., Einarsson, A., Siebert, C., Gislason, S.R., Halliday, A.N., 2011. Quantifying the impact of freshwater diatom productivity on silicon isotopes and silicon fluxes: Lake Myvatn, Iceland. Earth Planet. Sci. Lett. 305, 73–82.
Piper, B.S., Plinston, D.T., Sutcliffe, J.V., 1986. The water balance of Lake Victoria. Hydrolog. Sci. J. 31, 25–37.
Polissar, P.J., Abbott, M.B., Shemesh, A., Wolfe, A.P., Bradley, R.S., 2006. Holocene hydrologic balance of tropical South America from oxygen isotopes of lake sediment opal, Venezuelan Andes. Earth Planet. Sci. Lett. 242, 375–389.
Rozanski, K., Araguas-Araguas, L., Gonfiantini, R., 1996. Isotope patterns of precipitation in the East African region. In: Johnson, T.C., Odada, E.O. (Eds.), The Limnology, Climatology and Paleoclimatology of the East African Lakes. Gordon and Breach Publishers, Amsterdam, The Netherlands, pp. 79–93.
Rozanski, K., Araguás-Araguás, L., Gonfiantini, R., 1993. Isotopic patterns in modern global precipitation. In: Swart, P.K., Lohmann, K.C., McKenzie, J., Savin, S. (Eds.), Climate Change in Continental Isotopic Records. AGU, Washington, D.C, pp. 1–36.
Russell, J.M., Johnson, T.C., 2005. A high resolution geochemical record from Lake Edward, Uganda Congo and the timing and causes of tropical African drought during the late Holocene. Quat. Sci. Rev. 24, 1375–1389.
Russell, J.M., Johnson, T.C., 2006. The water balance and stable isotope hydrology of Lake Edward, Uganda-Congo. J. Gt. Lakes Res. 32, 77–90.
Russell, J.M., Johnson, T.C., 2007. Little Ice Age drought in equatorial Africa: Intertropical Convergence Zone migrations and El Niño-Southern Oscillation variability. Geology 35, 21–24.
Russell, J.M., Johnson, T.C., Kelts, K.R., Lærdal, T., Talbot, M.R., 2003a. An 11000-yr lithostratigraphic and paleohydrologic record from equatorial Africa: Lake Edward, Uganda-Congo. Palaeogeogr. Palaeoclimatol. Palaeoecol. 193, 25–49.
Russell, J.M., Johnson, T.C., Talbot, M.R., 2003b. A 725 yr cycle in the climate of central Africa during the late Holocene. Geology 31, 677–680.
Russell, J.M., Kelts, K.R., 1999. The sedimentologic history of Lake Edward, Uganda. IDEAL Bulletin (Summer), pp. 1–3.
Russell, J.M., Werne, J.P., 2009. Climate change and productivity variations recorded by sedimentary sulfur in Lake Edward, Uganda/D.R. Congo. Chem. Geol. 264, 337–346.
Schiff, C.J., Kaufman, D.S., Wolfe, A.P., Dodd, J., Sharp, Z.D., 2009. Late Holocene storm trajectory changes inferred from the oxygen isotope composition of lake diatoms, south Alaska. J. Paleolimnol. 41, 189–208.
Schlesinger, W., Bernhardt, E.S., 2013. Biogeochemistry: an Analysis of Global Change, third ed. Academic Press, Oxford.
Schlüter, T., 2008. Geological Atlas of Africa: with Notes on Stratigraphy, Tectonics, Economic Geology, Geohazards, Geosites and Geoscientific Education of Each Country, second ed. Springer-Verlag, Berlin.
Sharpley, A.N., Hedley, M.J., Sibbesen, E., Hillbricht-Ilkowska, A., Housw, W.A., Ryskowski, L., 1995. Phosphorus transfers from terrestrial to aquatic ecosystems. In: Tiessen, H. (Ed.), Phosphorus in the Global Environment. Wiley, Chichester, pp. 171–199.
Shemesh, A., Burckle, L.H., Hays, J.D., 1995. Late Pleistocene oxygen isotope records of biogenic silica from the Atlantic sector of the Southern Ocean. Paleoceanography 10, 179–196.
Smetacek, V., 1999. Diatoms and the ocean carbon cycle. Protist 150, 25–32.
Smil, V., 2000. Phosphorus in the environment: natural flows and human interferences. Annu. Rev. Energy Environ. 25, 53–88.
Smittenberg, R.H., Baas, M., Schouten, S., Sinninghe Damsté, J.S., 2005. The demise of the green alga *Botryococcus braunii* from a Norwegian fjord was due to early eutrophication. Holocene 133–140.
Sommer, M., Kaczorek, D., Kuzyakov, Y., Breuer, J., 2006. Silicon pools and fluxes in soils and landscapes - a review. J. Plant Nutr. Soil Sci. 169, 310–329.
Song, Z., Wang, H., Strong, P.J., Li, Z., Jiang, P., 2012. Plant impact on the coupled terrestrial biogeochemical cycles of silicon and carbon: implications for biogeochemical carbon sequestration. Earth Sci. Rev. 115, 319–331.
Spigel, R.H., Coulter, G.W., 1996. Comparison of hydrology and physical limnology of the East African Great Lakes: Tanganyika, Malawi, Victoria, Kivu and Turkana (with references to some of the North American Great Lakes). In: Johnson, T.C., Odada, E.O. (Eds.), The Limnology, Climatology and Paleoclimatology of the East African Lakes. Gordon and Breach, Amsterdam, pp. 102–135.
Stager, J.C., 1984. The diatom record of Lake Victoria (East Africa): the last 17,000 years. In: Mann, D.G. (Ed.), Proceedings of the Seventh Diatom Symposium, August 1982, Philadelphia, pp. 455–476.
Stager, J.C., Cumming, B., Meeker, L., 1997. A high-resolution 11,400-yr diatom record from Lake Victoria, East Africa. Quat. Res. 47, 81–89.
Stager, J.C., Cumming, B.F., Meeker, L.D., 2003. A 10,000-year high-resolution diatom record from Pilkington Bay, Lake Victoria, East Africa. Quat. Res. 59, 172–181.
Stager, J.C., Johnson, T.C., 2000. A 12,400 ^{14}C yr offshore diatom record from east central Lake Victoria, East Africa. J. Paleolimnol. 23, 373–383.
Stager, J.C., Johnson, T.C., 2008. The late Pleistocene desiccation of Lake Victoria and the origin of its endemic biota. Hydrobiologia 596, 5–16.
Stager, J.C., Mayewski, P.A., Meeker, L.D., 2002. Cooling cycles, Heinrich event 1, and the desiccation of Lake Victoria. Palaeogeogr. Palaeoclimatol. Palaeoecol. 183, 169–178.

Stager, J.C., Reinthal, P.N., Livingstone, D.A., 1986. A 25,000-year history for Lake Victoria, East Africa, and some comments on its significance for the evolution of cichlid fishes. Freshw. Biol. 16, 15–19.
Stager, J.C., Ryves, D.B., Chase, B.M., Pausata, F.S.R., 2011. Catastrophic drought in the Afro-Asian monsoon region during Heinrich Event 1. Science 331, 1299–1302.
Stallard, R.F., 1995. Tectonic, environmental and human aspects of weathering and erosion: a global review using a steady-state perspective. Annu. Rev. Earth Planet. Sci. 23, 11–39.
Stephens, T.W., 2011. A Diatom Stable Isotope Paleolimnology of Lake Pupuke (Ph.D. thesis). University of Auckland, Auckland, New Zealand.
Stone, J.R., Westover, K.S., Cohen, A.S., 2011. Late Pleistocene paleohydrography and diatom paleoecology of the central basin of Lake Malawi, Africa. Palaeogeogr. Palaeoclimatol. Palaeoecol. 303, 51–70.
Street-Perrott, F.A., 1995. Natural variability of tropical climates on 10- to 100-year time scales: limnological and palaeolimnological evidence. In: Martinson, D.G., Bryan, K., Ghil, M., Hall, M.M., Karl, T.R., Sarachik, E.S., Sorooshian, S., Talley, L.D. (Eds.), Natural Climate Variability on Decade-to-Century Time Scales. National Academy Press, Washington, D.C, pp. 506–511.
Street-Perrott, F.A., Barker, P.A., 2008. Biogenic silica: a neglected component of the coupled global continental biogeochemical cycles of carbon and silicon. Earth Surf. Process. Landf. 33, 1436–1457.
Street-Perrott, F.A., Barker, P.A., Leng, M.J., Sloane, H.J., Wooller, M.J., Ficken, K.J., Swain, D.L., 2008. Towards an understanding of late Quaternary variations in the continental biogeochemical cycle of silicon: multi-isotope and sediment-flux data for Lake Rutundu, Mt Kenya, East Africa, since 38 ka BP. J. Quat. Sci. 23, 375–387.
Street-Perrott, F.A., Barker, P.A., Swain, D.L., Ficken, K.J., Wooller, M.J., Olago, D.O., Huang, Y., 2007. Late Quaternary changes in ecosystems and carbon cycling on Mt. Kenya, East Africa: a landscape-ecological perspective based on lake-sediment fluxes. Quat. Sci. Rev. 26, 1838–1860.
Street-Perrott, F.A., Harrison, S.P., 1985. Lake levels and climate reconstruction. In: Hecht, A.D. (Ed.), Paleoclimate Analysis and Modeling. Wiley, New York, pp. 291–340.
Street-Perrott, F.A., Perrott, R.A., 1990. Abrupt climate fluctuations in the tropics: the influence of Atlantic Ocean circulation. Nature 343, 607–612.
Street-Perrott, F.A., Perrott, R.A., 1993. Holocene vegetation, lake levels, and climate of Africa. In: Wright, H.E.J., Kutzbach, J.E., Webb, T.I., Ruddiman, W.F., Street-Perrott, F.A., Bartlein, P.J. (Eds.), Global Climates Since the Last Glacial Maximum. University of Minnesota Press, Minneapolis, pp. 318–356.
Struyf, E., Conley, D.J., 2012. Emerging understanding of the ecosystem silica filter. Biogeochemistry 107, 9–18.
Struyf, E., Mosimane, K., Van Pelt, D., Murray-Hudson, M., Meire, P., Frings, P., Wolski, P., Schaller, J., Gondwe, M.J., Schoelynck, J., Conley, D., 2015. The role of vegetation in the Okavango Delta silica sink. Wetlands 35, 171–181.
Struyf, E., Smis, A., Van Damme, S., Garnier, J., Govers, G., Van Wesemael, B., Conley, D.J., Batelaan, O., Frot, E., Clymans, W., Vandevenne, F., Lancelot, C., Goos, P., Meire, P., 2010. Historical land use change has lowered terrestrial silica mobilization. Nat. Commun. 1, 129.
Stuiver, M., Reimer, P.J., Reimer, R.W., 2012. CALIB 6.0.
Sutcliffe, J.V., 2009. The hydrology of the Nile Basin. In: Dumont, H.J. (Ed.), The Nile: Origin, Environments, Limnology and Human Use. Springer Science + Business Media B.V, pp. 335–364.
Sutcliffe, J.V., Parks, Y.P., 1999. The Hydrology of the Nile. IAHS Special Publications. International Association of Hydrological Sciences Press, Wallingford, UK.
Swann, G.E.A., Leng, M.J., Juschus, O., Melles, M., Brigham-Grette, J., Sloane, H.J., 2010. A combined oxygen and silicon diatom isotope record of Late Quaternary change in Lake El'gygytgyn, North East Siberia. Quat. Sci. Rev. 29, 774–786.
Talbot, M.R., Lærdal, T., 2000. The Late Pleistocene-Holocene palaeolimnology of Lake Victoria, East Africa, based upon elemental and isotopic analyses of sedimentary organic matter. J. Paleolimnol. 23, 141–164.
Talbot, M.R., Livingstone, D.A., 1989. Hydrogen index and carbon isotopes of lacustrine organic matter as lake level indicators. Palaeogeogr. Palaeoclimatol. Palaeoecol. 70, 121–137.
Talbot, M.R., Williams, M.A.J., Adamson, D.A., 2000. Strontium isotope evidence for late Pleistocene reestablishment of an integrated Nile drainage network. Geology 28, 343–346.
Taylor, D., Robertshaw, P., Marchant, R.A., 2000. Environmental change and political-economic upheaval in precolonial western Uganda. Holocene 10, 527–536.
Theissen, K.M., Zinniker, D.A., Moldowan, J.M., Dunbar, R.B., Rowe, H.D., 2005. Pronounced occurrence of long-chain alkenones and dinosterol in a 25,000-year lipid molecular fossil record from Lake Titicaca, South America. Geochim. Cosmochim. Acta 69, 623–636.
Tierney, J.E., Russell, J.M., Sinninghe Damsté, J.S., Huang, Y., Verschuren, D., 2011. Late Quaternary behavior of the East African monsoon and the importance of the Congo Air Boundary. Quat. Sci. Rev. 30, 798–807.
Vandevenne, F.I., Delvaux, C., Hughes, H.J., Andre, L., Ronchi, B., Clymans, W., Barao, L., Govers, G., Meire, P., Struyf, E., 2015. Landscape cultivation alters δ^{30}Si signature in terrestrial ecosystems. Sci. Rep. 5.
Varela, D.E., Pride, C.J., Brzezinski, M.A., 2004. Biological fractionations of silicon isotopes in southern ocean surface waters. Glob. Biogeochem. Cycles 18, GB1047.
Viner, A.B., 1977. The sediments of Lake George (Uganda). IV: vertical distribution of chemical features in relation to ecological history and nutrient recycling. Arch. Hydrobiol. 80, 40–69.
Viner, A.B., Smith, I.B., 1973. Geographical, historical, and physical aspects of Lake George. Proc. R. Soc. Lond. Ser. B Biol. Sci. 184, 235–270.
von Blanckenburg, F., Bouchez, J., Ibarra, D.E., Maher, K., 2015. Stable runoff and weathering fluxes into the oceans over Quaternary climate cycles. Nat. Geosci. 8, 538–542.
White, F., 1983. The Vegetation of Africa. A Descriptive Memoir to Accompany the UNESCO/AETFAT/UNSO Vegetation Map of Africa. UNESCO, Paris.
Williams, M., Talbot, M., Aharon, P., Salaam, Y.A., Williams, F., Brendeland, K.I., 2006. Abrupt return of the summer monsoon 15,000 years ago: new supporting evidence from the lower White Nile valley and Lake Albert. Quat. Sci. Rev. 25, 2651–2665.
Williams, M.A.J., Adamson, D., Cock, B., McEvedy, R., 2000. Late Quaternary environments in the White Nile region, Sudan. Glob. Planet. Change 26, 305–316.
Williams, M.A.J., Usai, D., Salvatori, S., Williams, F.M., Zerboni, A., Maritan, L., Linseele, V., 2015. Late Quaternary environments and prehistoric occupation in the lower White Nile valley, central Sudan. Quat. Sci. Rev. http://dx.doi.org/10.1016/j.quascirev.2015.03.007.
Xu, Y., Jaffé, R., 2009. Geochemical record of anthropogenic impacts on Lake Valencia, Venezuela. Appl. Geochem. 24, 411–418.
Yool, A., Tyrrell, T., 2003. Role of diatoms in regulating the ocean's silicon cycle. Glob. Biogeochem. Cycles 17, 1103.
Zhang, Z., Zhao, M., Yang, X., Wang, S., Jiang, X., Oldfield, F., Eglinton, G., 2004. A hydrocarbon biomarker record for the last 40 kyr of plant input to Lake Heqing, southwestern China. Org. Geochem. 35, 595–613.
Zheng, Y., Zhou, W., Meyers, P.A., Xie, S., 2007. Lipid biomarkers in the Zoigê-Hongyuan peat deposit: indicators of Holocene climate changes in West China. Org. Geochem. 38, 1927–1940.